Foot And Ankle Injuries In Variable Energy Impacts

Kathryn Gallenberger
Marquette University

FOOT AND ANKLE INJURIES IN VARIABLE ENERGY IMPACTS

by

Kathryn A. Gallenberger, B.A.

A Thesis submitted to the Faculty of the Graduate School,
Marquette University,
in Partial Fulfillment of the Requirements for
the Degree of Master of Science

Milwaukee, Wisconsin

May 2013

ABSTRACT
FOOT AND ANKLE INJURIES IN VARIABLE ENERGY IMPACTS

Kathryn A. Gallenberger, B.A.

Marquette University, 2013

A total of 60 pendulum impacts to the plantar surface of 15 lower limb PMHS were conducted. Impact conditions were chosen to obtain data from high velocity tests without injury to model an under-vehicle landmine blast. For 19 impacts the specimen was initially positioned in 20-deg of dorsiflexion. The remaining impacts used neutral positioning.

The foot and ankle response was investigated based on impact energy and velocity. Response was characterized by heel pad and ankle joint stiffness. For neutral tests, axial force vs. compression corridors were developed for 2-3 m/s, 4-6 m/s, and 7-63 J impacts. For dorsiflexion tests corridors of 1-3 m/s, 6-8 m/s, 7-20 J, and 80-100 J were developed. These results indicate foot and ankle response is not more sensitive to impact energy than velocity. Lower limb manikins should be sensitive to both heel pad and ankle joint stiffness.

Fourteen calcaneus fractures and two tibia fractures were observed. Injury risk curves were developed for both neutral and dorsiflexion positioning using logistic regression. Strain gage data were used to obtain uncensored force values. In neutral, 50% probability of injury occurred at tibia axial force of 6800 N. In dorsiflexion, 50% probability occurred at 7900 N, but the regression was not statistically significant. These preliminary results indicate dorsiflexed specimens fracture at a higher force than neutral specimens.

ACKNOWLEDGMENTS

Kathryn A. Gallenberger, B.A.

This research was funded in part by the Department of Veterans Affairs Medical Center Research Service and by cooperative agreement W81XHW-10-2-0065 with the United States Army.

In no particular order, I would like to thank Dr. Pintar and my committee for their assistance, Michael Schlick and the staff of the Neuroscience Research Facility for their help in conducting the experiments, Dr. Emily Exten for her help with injury identification, and my family and friends for their encouragement.

TABLE OF CONTENTS

LIST OF TABLES

LIST OF FIGURES

I. INTRODUCTION

In the 1990s, concern over the long-term effects of lower extremity injury from vehicle collisions increased as a result of decreased fatalities following improved safety mechanisms for the head and thorax (Crandall et al., 1996). Currently, injuries to the foot and ankle are of concern for military personnel involved in under-vehicle landmine blasts.

When a landmine detonates below a vehicle, the floorplate of the vehicle is accelerated upwards and contacts the bottom surface of the foot (NATO Research and Technology Organization, 2007). The occupant's foot, ankle, and leg are closest to the detonation, and thus, the first to be loaded (NATO Research and Technology Organization, 2007). The loading in an underbody landmine blast is characterized by high amplitude and short duration (McKay & Bir, 2009). Average floor acceleration exceeds 100 g's and average peak Δv reaches 12 m/s (Wang, Bird, Swinton, & Krstic, 2001). Loading of the lower limb occurs 5-25 ms after detonation with peak tibial axial force occurring within the first 10 ms (NATO Research and Technology Organization, 2007). Studies performed on post-mortem human subjects (PMHS) under conditions characteristic of the automotive environment have applications to the under-vehicle blast environment; the effects of the floorplate acceleration on the occupant after landmine detonation are similar to the effects of footwell intrusion after a frontal vehicle collision (NATO Research and Technology Organization, 2007).

Lower extremity injuries are often not life-threatening but can lead to long-term disability or impairment, which in turn decreases occupational productivity of the injured

person (Kitagawa, Ichikawa, King, & Levine, 1998). Recently, improvised explosive devices or landmines caused 38% of the extremity wounds to soldiers in Operation Iraqi Freedom and Operation Enduring Freedom from October 2001 through January 2005 (McKay & Bir, 2009; Owens, Kragh, Macaitis, Svoboda, & Wenke, 2007). Of all wounds reported, 26% were to the lower extremity (Owens et al., 2007). Fractures of the foot accounted for 25% of lower extremity fractures, while the tibia and fibula were the most commonly fractured bones of the lower extremity (Owens et al., 2007). Refining the current understanding of foot and ankle response to dynamic impacts obtained from investigations in the automotive environment can aid the effort to mitigate foot and ankle injuries to military personnel resulting from under-vehicle landmine blasts.

II. FOOT AND ANKLE ANATOMY

The human foot and ankle contains 26 bones as well as numerous joints, tendons, ligaments, and muscles (Drake, Vogl, Mitchell, Gray, & Gray, 2010). The bones of the foot are divided into three groups: tarsals, metatarsals, and phalanges, as shown in Figure 1 (Drake et al., 2010). While the tibia and fibula, the medial and lateral long bones of the lower leg respectively, are not considered part of the foot and ankle region, they do have articulations with the proximal tarsal bones (Sanders & Walling, 2007). The tarsal bones form the skeletal structure of the ankle joint (Drake et al., 2010). The metatarsal and phalange bones form medial and lateral longitudinal arches and a transverse arch supported by muscles in the feet (Drake et al., 2010). The arches are important in walking and standing (Drake et al., 2010).

The tarsal bones are further divided into proximal, intermediate, and distal groups, which include the calcaneus and talus; navicular; and cuboid and cuneiforms, respectively (Drake et al., 2010). The proximal tarsal bones are also known as the hind foot (Drake et al., 2010; Funk, 2011). The calcaneus supports the talus and extends behind it to form the structural support of the heel (Drake et al., 2010). The calcaneus is an irregular box-shaped bone with six surfaces (Drake et al., 2010; Sanders & Clare, 2007). The superior surface has anterior, middle, and posterior facets that articulate with the talus, while the anterior surface articulates with the cuboid (Sanders & Clare, 2007). The lateral surface has grooves for the peroneal tendons and is the origin of the calcaneofibular ligament (Sanders & Clare, 2007). The medial surface includes the sustentaculum tali, a projection that supports the talar neck and is stabilized by the deltoid ligament (Drake et al., 2010; Sanders & Clare, 2007). The inferior surface has a

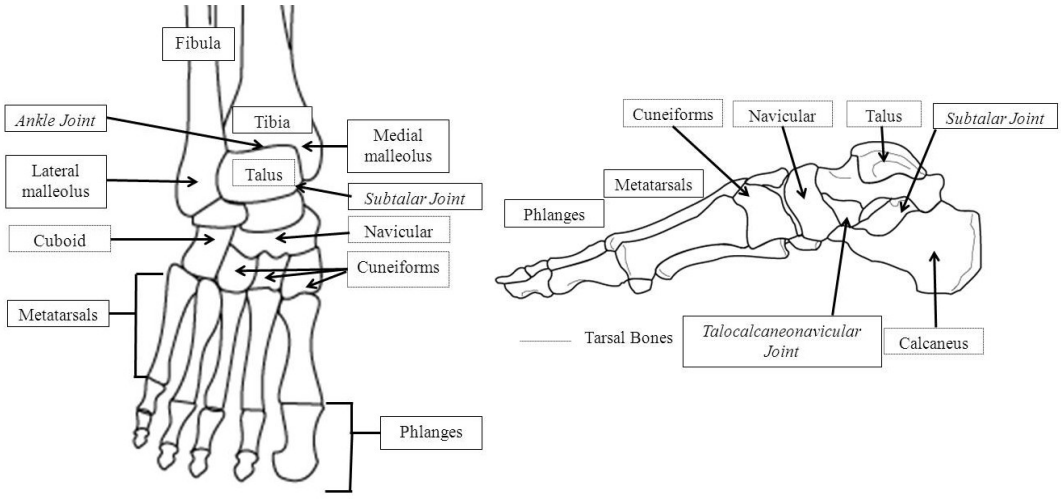

Figure 1: Anterior (left) and medial (right) views of foot and ankle anatomy

tuberosity to support the insertion of the Achilles' tendon (Sanders & Clare, 2007). Lastly, the posterior surface is weight-bearing (Drake et al., 2010; Khan, Oragui, & Akagha, 2010).

The other proximal bone, the talus, is comprised of a head, neck, and body (Drake et al., 2010) with five articulation surfaces that all bear weight (Sanders & Lindvall, 2007). Thus, 66.67% of the surface is covered with articular cartilage, and there are no tendon or muscle attachments (Sanders & Lindvall, 2007). The domed head articulates with the calcaneus via the middle and anterior facets inferiorly and with the navicular anteriorly (Drake et al., 2010). The body articulates superiorly with the inferior tibia, distal portion of the tibia (medial malleolus), and distal portion of the fibula (lateral malleolus) (Drake et al., 2010). The inferior surface of the body articulates with the calcaneus by the posterior facet (Drake et al., 2010). The neck does not have an articulation (Sanders & Lindvall, 2007). Since the talus connects the foot to the leg, it

transmits forces between the two body segments (NATO Research and Technology Organization, 2007).

The navicular, the intermediate tarsal bone, is located next to the cuboid on the medial side of the foot (Drake et al., 2010) and is a key portion of the medial longitudinal arch (Sanders & Papp, 2007). In addition to the talar head, it also articulates with the lateral cuneiform and cuboid (Sanders & Papp, 2007). The navicular has ample articular cartilage to support these articulations and a tuberosity for the insertion of the tibialis posterior tendon (Drake et al., 2010; Sanders & Papp, 2007).

In the distal portion, the cuboid is located on the lateral side of the foot and articulates with the calcaneus, navicular, lateral cuneiform, and lateral two metatarsals (Drake et al., 2010). On the medial side, each cuneiform articulates with neighboring cuneiform(s), the navicular, and one of the three most medial metatarsals (Drake et al., 2010). Together, the intermediate and distal tarsal bones are known as the midfoot (Drake et al., 2010; Funk, 2011).

Each of the five metatarsal bones and the fourteen phalanges is comprised of a distal head, shaft, and a proximal base (Drake et al., 2010). Each toe, except the big toe, contains a proximal, middle, and distal phalange (Drake et al., 2010). The phalanges are shorter than their corresponding metatarsal bone (Drake et al., 2010). The head or each metatarsal articulates with the proximal phalange of one toe, while the base articulates with at least one of the distal tarsal bones (Drake et al., 2010). The head of the distal phalange has no articulation (Drake et al., 2010). The metatarsals and phalanges comprise the forefoot (Drake et al., 2010; Funk, 2011).

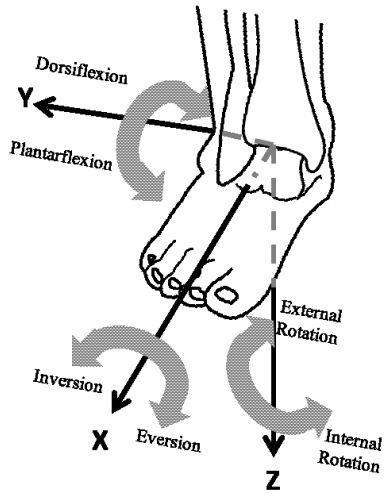

Figure 2: Rotations of the foot relative to the lower leg

The joints formed by the articulations of the bones in the foot allow many complex motions. Figure 2 illustrates the primary rotations of the foot and ankle complex. The angle of rotation is commonly measured by the angle of the calcaneus or forefoot relative to the tibia (Funk, 2011). In this illustration, inversion and eversion are rotations about the x-axis. Inversion and eversion are collectively referred to as xversion (Funk, 2011). The x-axis originates at the ankle joint and travels out the toes. Dorsiflexion and plantarflexion are rotations about the y-axis. The y-axis originates from the ankle joint and travels toward the medial portion of the ankle. Finally, internal and external rotations occur about the z-axis, which originates at the ankle joint and travels out the heel. Supination is often used to refer to inversion, and pronation is often used to refer to eversion (Funk, 2011). Supination and pronation can also refer to a combination of the rotations described above (Funk, 2011).

The distal tibia, distal fibula, and talus form the ankle joint. It is a synovial hinge joint that primarily allows dorsiflexion and plantarflexion (Drake et al., 2010; Huelke, 1986; Sanders & Clare, 2007). The ankle joint experiences the highest loads of all the

joints in the body and is most stable in dorsiflexion (Khan et al., 2010). It is stabilized by the deltoid and lateral ligament (Walling & Sanders, 2007). The lateral ligament complex is comprised of the anterior talofibular ligament, calcaneofibular ligament, and posterior talofibular ligament (Walling & Sanders, 2007).

The subtalar joint is comprised of the posterior facets of the calcaneus and talus (Drake et al., 2010). It allows gliding and rotation for xversion (Drake et al., 2010). It is stabilized by the bony structure as well as the calcaneofibular and talocalcaneal ligaments (Bellabarba, Barei, & Sanders, 2007). The subtalar joint allows the talus to rotate with the leg while the foot conforms to the surface with which it is in contact (Khan et al., 2010).

The articulation of the anterior and middle facets of the talus and calcaneus as well as the talar head-navicular articulation form the talocalcaneonavicular joint (Drake et al., 2010). It allows gliding and rotation for pronation and supination and is reinforced by the interosseous talocalcaneal, talonavicular, plantar calcaneonavicular, and the bifurcate ligaments (Drake et al., 2010). With the calcaneocuboid joint it is known as the transverse tarsal joint (Drake et al., 2010). The calcaneocuboid joint allows xversion as well as pronation and supination. It is supported by the bifurcate, long plantar and plantar calcaneocuboid ligaments (Drake et al., 2010).

III. PREVIOUS BIOMECHANICAL RESEARCH

Lower limb post-mortem human subjects (PMHS) have been loaded in a variety of directions using various devices. Lauge-Hanson (1950) conducted PMHS tests in a variety of loading conditions to investigate the resulting progression of soft tissue and bony injuries. He tested specimens in initial supination with forced adduction or eversion and in initial pronation with forced abduction or eversion (Lauge-Hansen, 1950). From these experiments he was able to identify the sequence of injuries occurring as each loading mode became more severe (Lauge-Hansen, 1950).

Since the 1990s the majority of the experimentalists have chosen conditions in xversion, dorsiflexion, and axial loading modes to model foot and ankle injuries in the automotive environment (Begeman & Prasad, 1990; Begeman, Balakrishnan, Levine, & King, 1993; Begeman & Aekbote, 1996; Crandall et al., 1996; Funk, Tourret, George, & Crandall, 2000; Funk, Srinivasan et al., 2002; Funk, Crandall et al., 2002; Jaffredo, Potier, Robin, Le Coz, & Lassau, 2000; Kitagawa, Ichikawa, King, & Levine, 1998; Klopp et al., 1997; Manning, Wallace, Roberts, Owen, & Lowne, 1997; Manning et al., 1998; McKay & Bir, 2009; McMaster et al., 2000; Parenteau, Viano, & Lovsund, 1995; Petit et al., 1996; Portier, Petit, Trosseille, Tarriere, & Lavaste, 1995; Portier et al., 1997; Rudd, Crandall, Millington, Hurwitz, & Hoglund, 2004; Schueler, Mattern, Zeidler, & Scheunert, 1995; Yoganandan et al., 1996; Yoganandan et al., 1999).

Some experiments to examine mechanisms of injuries to the foot and ankle were also conducted to re-produce specific fracture patterns or soft tissue injuries that have been seen clinically due to falls or sports injuries (Boon, Smith, Zobitz, & Amrami, 2001;

Carr, Hamilton, & Bear, 1989). These experiments are included in this review because of the available injury data.

Recently, researchers have begun conducting blast tests using PMHS and/or manikins to study the underbody blast environment (Bir et al., 2008; Bird, 2001; Geurts et al., 2006; Horst, Simms, Maasdam, & Leerdam, 2005; Pandelani, Reinecke, Philippens, Dosquet, & Beetge, 2010; Wang, Bird, Swinton, & Krstic, 2001; Wolff et al., 2005). Only the study by McKay and Bir (2009) was included in this review because the methods used were similar to the automotive studies.

A. SPECIMEN DETAILS

In most test series, more male specimens were tested than female specimens. However, axial impacts performed by Kitagawa et al. (1998) tested more female specimens than male, with twelve females compared to four males. Begeman and Prasad (1990), Schueler et al. (1995), and Yoganandan et al. (1996, 1999) tested specimens with average ages from 37-52 years, while the 12 other studies had average ages ranging from 60-78 years. To properly reflect the military population, mostly young male specimens should be tested. According to the Department of Defense, in 2011 83% of non-prior service active personnel were male, and 92% were 17-25 years old (Office of the Under Secretary of Defense, 2011). Availability of specimens may limit the ability to use a sample reflective of the age of military personnel.

Only Portier et al. (1997) and Schueler et al. (1995) used whole body PMHS. Using a whole body specimen accurately reflect the effects of more proximal body segments on the foot and ankle response. In preparation for the other dynamic impacts, PMHS were sectioned in numerous locations, including mid-femur, mid-tibia and -fibula, and at the knee. Since occupants are seated in automobiles and military vehicles, the torso is of less interest than the lower limb. Sectioning at the mid-femur leaves the knee joint intact, which allows movement after impact. Funk et al. (2000) and Klopp et al. (1997) used a femur bar to re-create the original hip-to-knee length of the specimen. McKay and Bir (2009) simulated the presence of the whole body by attaching the specimen to a Hybrid III manikin. In some cases, the knee was fixed to model knee entrapment (Funk et al., 2000).

Sectioning the specimen below the knee removes the effects of the thigh's mass on response to the impact. To simulate the effects of more proximal body segments, some experimentalists introduced an axial pre-load of one-half body weight or 0.5-1.5kN prior to axial impacts (Boon et al., 2001; Funk, Crandall et al., 2002; Funk et al., 2000; Klopp et al., 1997; McMaster et al., 2000). Under xversion loading, Funk, Srinivasan et al. (2002) introduced pre-load of 2kN. Funk, Srinivasan et al. (2002) found a higher axial force as well as higher xversion moments and angles in the presence of a pre-load. Due to anatomic variability among subjects, each lower limb specimen had a different mass. Thus, Yoganandan et al. (1996, 1999) ballasted all specimens to 16 kg to obtain a consistent mass for the specimen assembly and to simulate the thigh mass.

Variable amounts of motion were permitted at the proximal tibia. Several studies used a potting procedure at the proximal tibia and then fixed the specimen to a rigid wall (Begeman and Aekbote, 1996; Kitagawa et al., 1998; McMaster et al. 2000). Axial tests by Yoganandan et al. (1996, 1999) as well as xversion tests by Funk, Srinivasan et al. (2002) permitted the specimen to translate after impact. Boundary conditions at the proximal tibia could affect resulting injuries.

The musculature in PMHS lacks the tension present in live subjects. In the automotive environment, tensioning of the Achilles' tendon can be associated with 'panic' braking (Kitagawa et al., 1998). Funk, Crandall et al. (2002) investigated the effect of Achilles' tension on the experimental outcome for axial loading. They found the presence of tensioning increased the average tibia axial force, which is a key factor in injury prediction under axial loading (Funk, Crandall et al., 2002). Furthermore, the distal tibia was fractured more often than the calcaneus (Funk, Crandall et al., 2002).

Variations in injury thresholds and injury locations in existing literature could result from the presence of Achilles' tension.

Load cells were placed at the proximal tibia after fixation material or implanted in the tibia after about 9 cm of bone was removed (Funk et al., 2000; Kitagawa et al., 1998; McKay & Bir, 2009; Portier et al., 1997; Yoganandan et al., 1996; Yoganandan et al., 1999). Other instrumentation, such as accelerometers, angular rate sensors, and acoustic emission sensors, were mounted to various bones including the calcaneus and tibia. In some cases, the hind foot or forefoot was fixed to the footplate through bones in the foot (Begeman and Aekbote, 1996; Hirsch and Lewis, 1965; Portier et al. 1997).

In the three studies using rigid fixation through the calcaneus, three calcaneus fractures occurred, which is the minority of injuries. One fracture was attributed to the fixation, while the effect of the fixation method on the other fractures was not mentioned. Similarly, Funk et al. (2000) as well as McKay and Bir (2009) discounted some fractures that occurred at the bone-potting interface for the load cell implanted mid-tibia. Fixing instrumentation directly to the bone with hardware or removing bone to implant a load cell could compromise the structure, thereby influencing fracture patterns. In bones where fracture is expected, it is preferable to use adhesives on the surface rather than rigid fixation through the structure to mount instrumentation to ensure resulting injuries reflect injuries seen in the field.

B. XVERSION LOADING

Together the four xversion loading studies conducted 45 inversion trials and 48 eversion trials (Begeman et al., 1993; Funk, Srinivasan et al., 2002; Petit et al., 1996; Parenteau et al., 1995). Thirty-three trials in inversion resulted in injury and 36 trials in eversion resulted in injury. The four studies performed an average of 23 trials. Details for the experimental set-up of xversion loading experiments are given in Table 1. The

Table 1: Experimental set-up for xversion loading studies

Xversion Loading Study	Specimen Preparation	Boundary Conditions	Initial Conditions	Apparatus	Input Angular Velocity
Begeman et al. (1993)	-Sectioned mid-tibia/fibula	-Proximal end fixed -Up to 10 cm footplate travel -Calcaneus fixed to footplate -Dorsi/ plantarflexion restricted	-Specimen horizontal -23-deg dorsiflexion, 13-deg plantarflexion, or foot 90-deg to tibia	-Pneumatic impactor -Impact aligned 5 cm from ankle joint	-2000 deg/s
Funk, Srinivasan et al. (2002)	-Sectioned distal of knee -Implanted load cell mid-tibia and mid-fibula -Instrumentation fixed to mid-foot	-Foot fixed to footplate -Free translation of proximal tibia	-Specimen horizontal or proximal tibia raised for 30-deg of dorsiflexion -Foot 90-deg to tibia or 14-deg of xversion -No axial pre-load or 2.0 kN axial pre-load	-Pneumatic impactor to guided cam	-1000 deg/s
Petit et al. (1996)*; Parenteau et al. (1995)*	-Sectioned mid-tibia/fibula -Calcaneus fixed	-Flat plate at proximal tibia translated -Rotation limited to 45-deg of xversion	-Specimen vertical -Foot 90-deg to tibia -0.4 kN Achilles' tension (Petit et al., 1996)	-Custom motor and gear box	-7 deg/s

*quasistatic loading

two dynamic studies used a pneumatic impactor to load the specimen at 1000 deg/s or 2000 deg/s (Begeman et al., 1993; Funk, Srinivasan et al., 2002). They also fixed the foot to the footplate. The quasistatic studies used a custom system with a motor and gear box to load specimens at 7 deg/s (Petit et al., 1996; Parenteau et al., 1995).

Begeman et al. (1993) and Funk, Srinivasan et al., (2002) introduced dorsiflexion or plantarflexion to the foot and ankle before the dynamic xversion loading. In contrast, Petit et al. (1996) and Parenteau et al. (1995) only tested specimens with the foot and ankle in neutral, where the foot is 90-deg to the tibia. Begeman et al. (1993) obtained the initial flexion positioning by rotating the foot relative to the tibia. Funk, Srinivasan et al. (2002) obtained initial dorsiflexion by raising the proximal tibia. The level of dorsiflexion was constant during application of the xversion load (Funk, Srinivasan et al., 2002). This positioning method allowed the foot to remain parallel to the footplate.

To characterize the response of the foot and ankle, moment vs. angle curves were created. When using data from injury tests, the response was only valid up to the point of injury (Funk, Srinivasan et al., 2002). Begeman et al. (1993) were able to compare the moment-angle response curves to data collected using the HybridIII manikin to ensure the HybridIII results were similar to the PMHS results. In Funk, Srinivasan et al.'s study (2002), the moment-angle response for specimens with 30-deg dorsiflexion was similar to the response seen in neutral specimens.

Data for xversion moment, axial force, and xversion angle from the tests resulting in injury are shown in Table 2. While not the primary loading direction, axial load was important due to Achilles' tensioning and axial pre-loading. Injuries occurred in

Table 2: Range of moment, angle, and force values measured in xversion loading tests

Study	Inversion			Eversion		
	Failure Moment (Nm)	Failure Angle (deg)	Maximum Axial Load (N)	Failure Moment (Nm)	Failure Angle (deg)	Maximum Axial Load (N)
Begeman et al. (1993)	21-40	50-65	350-850	18-55	50-67	530-800
Funk, Srinivasan et al. (2002)	15-117	27-44	0-3035	23-238	19-56	0-3208
Parenteau et al. (1995)*	17-51	26-42		36-60	25-39	
Petit et al. (1996)*	14-66	26-42		26-44	25-39	

*quasistatic loading

inversion at moments of 14-117 Nm, angles of 26-65-deg, and axial loads of 0-3035 N. In eversion, injuries occurred at moments of 18-238 Nm, angles of 19-67-deg, and axial loads of 0-3208 N. Injury threshold values are shown in Table 3.

Injury occurred at higher moments and angles in the presence of an axial pre-load. Malleolar fractures were the most common fracture for xversion loading (Begeman et al., 1993; Funk, Srinivasan et al., 2002). Both dynamic studies found talus fractures in specimens with initial dorsiflexion but not in specimens with neutral positioning (Begeman et al., 1993; Funk, Srinivasan et al., 2002). Malleolar fractures occurred in specimens under both conditions. Initial positioning of the specimen in dorsiflexion prior to xversion loading affected the injury outcome but not the moment-angle response.

Table 3: Angle and moment due to xversion loading for 50% probability of injury

Study		Inversion Moment (Nm)		Eversion Moment (Nm)		Xversion Angle (deg)	Measurement Location
		female	male	female	male		
Begeman et al. (1993)						58	Mid-tibia
Funk, Srinivasan et al. (2002)	Axial pre-load	43	56	82	106	41	Mid-tibia (implanted)
	No axial pre-load	23	31	43	58	33	

C. DORSIFLEXION LOADING

In addition to xversion loading, lower limb PMHS were also tested under dorsiflexion loading. The six studies consisted of 104 tests with 42 resulting in injury (Begeman and Prasad, 1990; Manning et al., 1998; Parenteau et al., 1995; Petit et al. 1996; Portier et al., 1997; Rudd et al., 2004). An average of 17 impacts was conducted for each study. Manning et al. (1997) performed 28 low energy impacts to five specimens, which allowed for paired tests. Other investigators performed one impact per specimen.

Dynamic dorsiflexion loads were generated by pendulums or linear impactors contacting the ball of the foot. Impact velocities included 3-8 m/s. Begeman and Prasad (1990) used a pendulum mass of 16.3 kg to generate impacts of 73-535 J. Manning et al. (1997) used a low mass pendulum of 1.5 kg and a high mass pendulum of unspecified mass. The low mass pendulum generated impact energies up to 27 J. Portier et al. (1995, 1997) used a sled to obtain impact velocities of 14.6-15.8 m/s. Quasistatic tests applied dorsiflexion rotation to the foot and ankle rather than using an axial load to induce rotation. The same apparatus was used as in the quasistatic xversion loading. Unlike the constant dorsiflexion angle used by Funk, Srinivasan et al. (2002) in xversion loading, the amount of dorsiflexion changed due to the impact.

Most investigators initially positioned the specimens in neutral. However, Portier et al. (1995, 1997) used "driver geometry." In driver geometry, the knee is in flexion and the foot is placed on a brake pedal to more accurately reflect posture when driving (Portier et al., 1995; Portier et al., 1997). In this configuration, the load path is not

parallel to the tibia (Portier et al., 1997). Details for all experimental set-ups are given in Table 4.

Table 4: Experimental set-up for dorsiflexion loading studies

Dorsiflexion Loading Study	Specimen Preparation	Boundary Conditions	Initial Conditions	Apparatus	Input Velocity & Input Energy
Begeman and Prasad (1990)	-Sectioned distal of knee -Instrumentation fixed to tibia and foot	-Proximal end fixed -25 mm Ensolite on impactor -Impactor aligned 62.5 mm anterior of ankle joint	-Specimen horizontal -Foot 90-deg to tibia	-Pneumatic impactor (16.3 kg) with 25 mm diameter	-3.0-8.1 m/s -73-535 J
Manning et al. (1997, 1998)	-Sectioned at knee -Implanted load cell mid-tibia -Instrumentation fixed to navicular and tibia	-PVC sheeting ("shoe sole") sutured to foot -Impact to forefoot	-Specimen horizontal -Foot 90-deg to tibia -1 kN Achilles' tension	-Pendulum (1.5 kg and "high"mass)	-2.0-6.0 m/s -12-27 J and N/A
Parenteau et al. (1995)*; Petit et al. (1996)*	-Sectioned mid-tibia/fibula -Calcaneus fixed	-Flat plate at proximal tibia translated -Rotation limited to 75-deg plantarflexion and 60-deg dorsiflexion	-Specimen vertical -Foot 90-deg to tibia -0.9 kN Achilles' tension (Petit et al., 1996)	-Custom motor and gear box	-7deg/s rotation -N/A
Portier et al. (1995, 1997)	-Full body PMHS -Implanted load cell mid-tibia -Distal tib/fib fixed	-Placed in car seat fixed to sled -Impact to forefoot	-Driver geometry	-Sled	-14.6-15.8 m/s -N/A
		-Placed with posterior in contact with floor -Impact to forefoot	-Lower leg horizontal -Foot 90-deg to tibia	-Spring and dashpot linear impactor -Impact to ball of foot	- ~5 m/s -N/A
Rudd et al. (2004)	-Sectioned mid-femur -Implanted load cells mid-tibia and mid-fibula -Instrumentation fixed to calcaneus	-Proximal end fixed -17 cm of footplate intrusion -Vertical support strap distal of knee -Femur 90-deg to tibia -Impact to forefoot	-Specimen horizontal -Foot 90-deg to tibia	-Pneumatic impactor	-3.1-6.9 m/s -N/A

*quasistatic loading

Table 4: Range of moment, angle, and force values measured in dorsiflexion loading tests

Study	Failure Moment (Nm)	Failure Angle (deg)	Maximum Axial Load (N)
Begeman and Prasad (1990)	70-210	57-70	1850-2900
Manning et al. (1998)	36	64	4605
Parenteau et al.(1995)*	16-50	33-55	
Petit et al. (1996)*	30-64	44-54	
Portier et al. (1995, 1997)	-52, 58-95	25-30	1650-3320
Rudd et al. (2004)	15-107	21-57	616-2563

*quasistatic loading

Injuries occurred at moments ranging from 36-210 Nm, dorsiflexion angles ranging from 25-70°, and axial loads ranging from 1650-4605 N. Injury values are shown in Table 4. Note that only one impact resulted in injury in the study by Manning et al. (1998). Manning et al. (1997) was able to use impact velocities up to 6 m/s with a 1.5 kg pendulum without creating an injury. They found applying Achilles' tension affected the resulting peak axial load and dorsiflexion angle but not the peak flexion moment (Manning et al., 1998).

Begeman and Prasad (1990) obtained moment vs. angle responses from non-injury impacts and compared the results to the response of a HybridIII manikin. Flexion moments measured in the HybridIII were higher than in the PMHS (Begeman & Prasad, 1990). From these data they were able to propose an ankle stiffness corridor for the HybridIII (Begeman & Prasad, 1990). Rudd et al. (2004) created characteristic moment vs. angle plots for PMHS response by fitting a second order polynomial to their data. The characteristic response of the Thor-Lx manikin was found using linear regression

from 0-31-deg and a second order polynomial for angles exceeding 31-deg (Rudd et al., 2004). They found the response of the Thor-Lx to be similar to the response of the PMHS up to 35-deg of dorsiflexion (Rudd et al., 2004). Characterizing the PMHS response is important to evaluating the biofidelity of a manikin.

Malleolus fractures were most common followed by talus fractures. Begeman and Prasad (1990) associated dorsiflexion angle of 45° with the injury threshold. Rudd et al. (2004) determined the risk of 50% injury at 51° of dorsiflexion and at 85 Nm of moment using data from a mid-tibia load cell and angular rate sensor. Kuppa et al. used data from Portier et al. (1997) to determine a 50% probability of AIS2+ injury at 60 Nm of flexion moment (Petit et al., 1996). These data were also collected mid-tibia (Portier et al., 1997). Since the threshold for injury in dorsiflexion is at about 50-deg, the initial 30-deg of dorsiflexion in Funk, Srinivasan et al.'s xversion loading study (2002) likely did not cause injury. In all studies, angle and moment were considered separately as predictors of injury.

D. AXIAL LOADING

In under-vehicle landmine blasts, the primary load to the foot and ankle is axial. The 12 studies reviewed using axial loading include a total of 370 impacts, of which 218 resulted in injury (Begeman and Aekbote, 1996; Boon et al., 2001; Carr et al., 1989; Funk et al. (2000); Funk, Crandall, et al., (2002); Hirsch and Lewis, 1965; Kitagawa et al., 1998; Klopp et al., 1997; McKay and Bir, 2009; McMaster et al., 2000; Schueler et al., 1995; Yoganandan et al., 1996; Yoganandan et al., 1999). The average sample size was 44. In some studies specimens that did not sustain an injury were re-tested (Begeman & Aekbote, 1996; Yoganandan et al., 1996).

To date, investigators have used 16-38 kg pendulums and pneumatic impactors at velocities of 2-12.5 m/s to generate axial impacts (Begeman and Aekbote, 1996; Funk et al., 2000; Funk, Crandall et al., 2002; Kitagawa et al., 1998; Klopp et al., 1997; McKay and Bir, 2009; McMaster et al., 2000; Schueler et al., 1995; Yoganandan et al., 1996; Yoganandan et al., 1999). Impact energies were reported from 60-3000 J.

Various other devices were used to axially load lower limb PMHS. In addition to a pneumatic impactor, Begeman and Aekbote (1996) used an electro-hydraulic testing device to axially load specimens. Boon et al. (2001) used a servohydraulic materials testing machine. The quasistatic tests performed by Hirsch and Lewis (1965) used a lever system. Lastly, Carr et al. (1989) created a dynamic impact by dropping a mass along a 150 cm guide rod, accelerating the mass to 5.4 m/s for impact to the proximal tibia.

The majority of experiments using axial loading initially placed the specimen in neutral, with the foot perpendicular to the tibia. Funk et al. (2000) and Klopp et al.

(1997) positioned the specimen in "driver geometry," similar to Portier et al. (1997) for dorsiflexion loading. Funk et al. (2000) and Klopp et al. (1997) used a pendulum impactor and a transfer piston with a universal joint insured the load was directed along the tibial axis. Table 6 fully details the experimental set-ups for the axial loading studies.

Some variability in initial positioning of the foot and ankle under axial loading is apparent in literature. Yoganandan et al. (1996) included tests that used 20-deg of initial dorsiflexion. Klopp et al. (1997) and Funk et al. (2000) initially positioned specimens in 10-deg of inversion/eversion and/or 0-30-deg of plantar/dorsiflexion. The angle of the footplate was adjusted to obtain initial rotation (Klopp et al., 1997). Initial rotation of the foot and ankle prior to impact was also introduced in the quasistatic tests performed by Hirsch and Lewis (1965).

In contrast to the axial studies with initial dorsiflexion, specimens loaded in dorsiflexion experienced significant dorsiflexion rotation during the impact event. Dorsiflexion loading experiments with neutral positioning and axial loading experiments with initial dorsiflexion positioning directed the load along or parallel to the tibial axis. The tibial axis was chosen for axial loading because Crandall et al. (1996) reported that the fibula sustains 7-12% of the axial load to a neutrally positioned foot.

Table 6: Experimental set-up for axial loading studies

Axial Loading Study	Specimen Preparation	Boundary Conditions	Initial Conditions	Apparatus	Input Velocity & Input Energy
Begeman and Aekbote (1996)	-Sectioned mid tibia/fibula	-Loading plate fixed to calcaneus -Proximal end fixed to rigid frame	-Specimen horizontal -Restraints positioned foot 90-deg to tibia	-Pneumatic impactor	-N/A
Boon et al. (2001)	-Sectioned proximal of ankle	-Foot fixed with plaster of Paris	-Specimen secured upright -900 N axial pre-load -10-deg inversion and 20-deg dorsiflexion with wedges	- MTS servohydraulic testing machine	-N/A
Carr et al. (1989)	-Sectioned distal of knee	-Distal end fixed	-Specimen secured upright -≤5-deg varus, valgus, equinas	-6.8-31.8 kg weights dropped ~1.5 m on guided rod to impact proximal tibia	-5.4 m/s (average) -100-468 J (based on average)
Funk et al. (2000); Funk, Crandall, et al. (2002); Klopp et al. (1997)	-Sectioned mid-femur -Implanted load cell mid-tibia -Instrumentation fixed to foot and/or tibia	-Proximal end fixed -≤ 16 cm of footplate intrusion (Funk et al., 2000) -Foam padding between foot and contact plate (Funk et al., 2000; Funk, Crandall et al., 2002) -Vertical straps supporting lower leg (Funk et al., 2000) -Femur 90-deg to tibia (Funk et al., 2000) -Knee constrained (Funk et al., 2000)	-Specimen horizontal (Funk et al., 2000; Funk, Crandall et al. 2002) or in driver geometry (Funk et al., 2000, Klopp et al., 1997) -One-half body weight axial pre-load -Neutral, 10-deg xversion and/or ≤ 30-deg dorsi/plantarflexion (Funk et al., 2000, Klopp et al., 1997) -1.0 kN Achilles' tension (Funk, Crandall et al. 2002)	-Pendulum (33 kg) to transfer piston	-2.0-7.0 m/s -100-800 J

Hirsch and Lewis (1965)*	-Sectioned distal of knee	-Proximal end and foot fixed	-Specimen secured upright -Pronation, supination, or 45-deg dorsi/plantarflexion with wooden blocks	-Custom lever system	-N/A
Kitagawa et al. (1998)	-Sectioned mid tibia/fibula	-Proximal end fixed	-Specimen horizontal - Foot 90-deg to tibia -1.0 kN Achilles' tension	-Pendulum (18 kg) -15 mm posterior of tibia axis	-2.4-4.0 m/s -50-140 J
McKay and Bir (2009)	-Sectioned mid-femur -Implanted load cell mid-tibia	-Femur attached to HybridIII manikin	-Specimen horizontal -Femur 90-deg to tibia -Foot 90-deg to tibia	-High-rate linear impactor (38.7 kg)	-7.0-12.0 m/s -950-2800 J
McMaster et al. (2000)	-Sectioned at knee	-3 mm thick rubber sheet between foot and impactor -Proximal end fixed	-Specimen horizontal -0.5-1.0 kN tibia pre-load -1.5-2.0 kN Achilles' tension	-Linear impactor -Variable alignment with tibia axis	-N/A
Schueler et al. (1995)	-Full body PMHS -Instrumentation fixed to tibia -Instrumented shoe	-Placed in suspended seat -Shoe on impacted foot	-Specimen lower leg horizontal -Foot 90-deg to tibia	-Pneumatic impactor (38 kg)	-6.7-12.5 m/s -845-2968 J
Yoganandan et al. (1996, 1999)	-Sectioned at knee -Ballasted to 16 kg	-Padding on pendulum face -Minisled with 2.5 m run-out	-Specimen horizontal -Foot 90-deg to tibia	-Pendulum (24 kg)	-2.2-7.6 m/s -59-540 J

*quasistatic loading

Input energies and velocities as well as tibia axial force are given in Table *5*. Tibia axial forces as high as 10,159 N were measured at the tibia without injury and as low as 1100 N with injury. Injuries occurred at energies and velocities as low as 2.37 m/s and 51 J, respectively. No injury was observed in impacts up to 11.3 m/s and 2462 J. Injury biomechanics appear to be dependent on experimental set-up. Kitagawa et al. (1998) impacted specimens with an 18 kg pendulum at about 3 m/s, producing calcaneus and tibia pylon fractures. Yoganandan et al. (1996) also conducted impacts at 3 m/s, but with a 24 kg pendulum. Most specimens did not sustain an injury at that level.

Each study in axial loading used one impactor mass. Thus, the energy ranges in these studies resulted from a constant mass and varied velocity. Since energy can be modulated by impactor mass and velocity, it more fully characterizes the impact conditions than velocity alone. In general, as impact velocity increased, the proportion of injury tests increased. Thus, lighter pendulums should be used to obtain data from non-injury impacts at higher velocities, similar to the study performed by Manning et al. (1997) with dorsiflexion loading.

Crandall et al. (1996) have presented the response of the foot and ankle to 5 m/s heel impacts and 6.5 m/s plantar impacts. A 15 kg pendulum was used for the 5 m/s impacts, resulting in an impact energy of 187 J. The response was given as compressive force vs. displacement. For the 5 m/s axial impacts, 1100 N of compressive force reflected 4.5 mm displacement. For 6.5 m/s impacts, 3500 N reflected 4.2 mm displacement (Crandall et al., 1996). No sub-injury response data is available for specimens with initial dorsiflexion or xversion.

Table 5: Summary of data from axial loading tests

Study	Velocity Input (m/s)		Energy Input (J)		Tibia Axial Force (N)	
	Highest Non-failure	Lowest Failure	Highest Non-failure	Lowest Failure	Highest Non-failure	Lowest Failure
Begeman and Aekbote (1996)					5650-8690	
					7440	6990
Boon et al. (2001)					1100-8900	
					4400	1100
Carr et al. (1989)			100-468			
			-	100		
Funk et al. (2000)	2.0-7.0		100-800		2707-7929^	
	N/A	N/A	N/A	N/A	N/A	2707
Funk et al. (2002)	5.0				2600-10,800	
	5.0	5.0			5263	2574
Hirsch and Lewis (1965)*					145-925 kp	
					-	145 kp
Kitagawa et al. (1998)	2.91-3.99		51-143		5737-9108	
	3.17	2.37	90	51	8152	5735
Klopp et al. (1997)					1783-10,866	
					7737	2707
McKay and Bir (2009)	6.8-12.2		857-2670		1360-9866	
	7.7	9.0	1089	1491	5858	1360
McMaster et al. (2000)					2723-10,713	
					10,197	2723
Schueler et al. (1995)	6.67-12.5		845-2966		7700-20,500	
	11.3	7.1	2426	958	20,400	7700
Yoganandan et al. (1996)	2.2-7.6		58-693		4328-13,000	
	7.6	3.4	462	145	10,159	4328

*quasistatic loading ^ failure values only

Funk, Crandall et al. (2002) used acoustic emission (AE) sensors and McKay and Bir (2009) used strain gages on the tibia and/or calcaneus to more precisely identify the time of fracture initiation. Funk, Crandall et al. (2002) found bursts of acoustic emission corresponded to local peak tibia axial force. McKay and Bir (2009) similarly found time of peak strain coincided with the time of peak tibia axial force. Thus, peak axial force was used to identify time of injury.

The distribution of fractures by loading mode is shown in Figure 3. Malleolus fractures are most common for the rotation loading modes (xversion and dorsiflexion), while calcaneus fractures are most common for axial loading. Under all three loading modes, talus, calcaneus, and malleolus fractures were the three most common. Tibia pylon fractures were only seen under axial loading. Tibia pylon fractures occur at the articular surface of the distal tibia with the talus, which is part of the ankle joint (Sanders and Walling, 2007). They are believed to be cause by an axial load in conjunction with initial dorsiflexion or plantarflexion (Sanders and Walling, 2007).

In some axial loading studies investigators controlled the level of intrusion. The experimental set-up used by Funk et al. (2000) allowed either 6 cm or 16 cm of intrusion. They found increased intrusion caused more malleolar fractures, while calcaneus fractures were more common at lower levels of intrusion (Funk et al., 2000). McKay and Bir (2009) allowed 24 mm of intrusion in their experimental set-up but did not produce any malleolar fractures (2009). From intrusion they were able to calculate compressive strain of the lower limb (McKay and Bir, 2009). They found compressive strain to be a significant ($p < 0.05$) predictor of injury but did not present sub-injury results (McKay & Bir 2009).

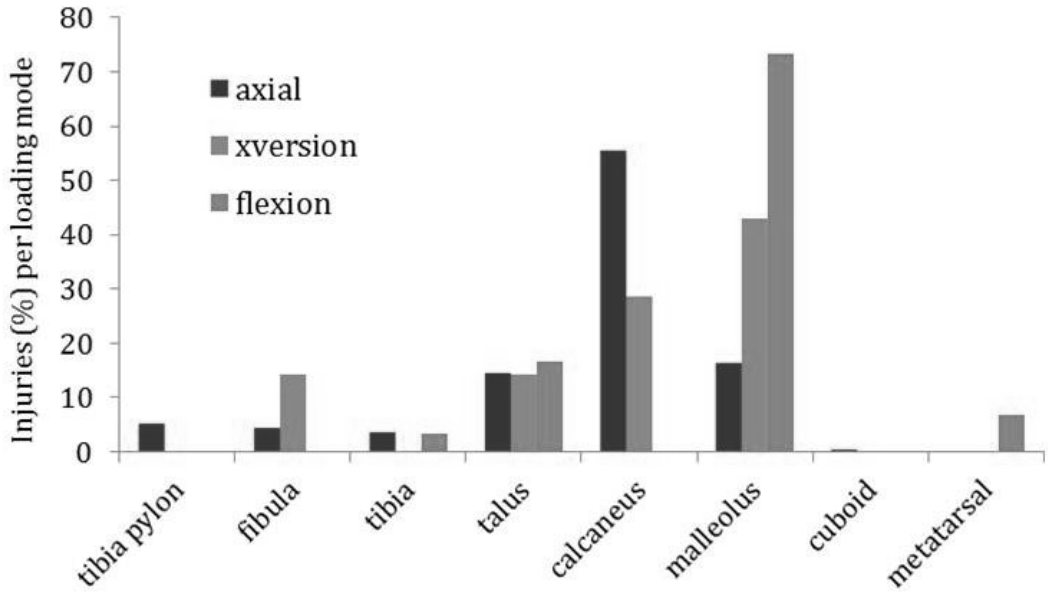

Figure 3: Fractures as % of total injuries from axial, xversion, and flexion loading (Begeman & Prasad, 1990; Begeman, Balakrishnan, Levine, & King, 1993; Begeman & Aekbote, 1996; Boon, Smith, Zobitz, & Amrami, 2001; Carr, Hamilton, & Bear, 1989; Funk, Tourret, George, & Crandall, 2000; Funk, Crandall et al., 2002; Funk, Srinivasan et al., 2002; Hirsch & Lewis, 1965; Kitagawa, Ichikawa, King, & Levine, 1998; Klopp et al., 1997; McKay & Bir, 2009; McMaster et al., 2000; Parenteau, Viano, & Lovsund, 1995; Portier et al., 1997; Rudd, Crandall, Millington, Hurwitz, & Hoglund, 2004; Schueler, Mattern, Zeidler, & Scheunert, 1995; Yoganandan, Pintar, Gennarelli, Seipel, & Marks, 1999)

Injury criteria developed for axial loading are shown in Table 6 and Table 9. All these criteria are based solely on tibia axial force. Furthermore, only Funk, Crandall et al. (2002) and McKay and Bir (2009) verified that injury occurred at peak tibia axial force. Klopp et al. (1997) were the only investigators to develop an injury criterion based on initial position. Initial xversion was not found to be a significant factor in predicting injury but initial dorsiflexion was (Klopp et al., 1997). For a footplate force of 8000 N, 50% risk of injury in dorsiflexion was at 60 rad/s, in neutral was at 45 rad/s, and in plantarflexion was at 29 rad/s (Klopp et al., 1997). The amount of dorsiflexion was not included as a factor in the injury criterion. More investigation is needed into identifying force at fracture and developing injury criterion for initially dorsiflexed specimens.

Table 6: Axial forces due to axial loading for 50% probability of injury by age and gender

Study	Age (years)	Size and Gender	Tibia Axial Force (N)	Measurement Location
Funk, Crandall et al. (2002)	45	50th M	8300	mid tibia (implanted)
	65	50th M	6100	
	45	5th F	5000	
	65	5th F	3700	
Yoganandan et al. (1996)	45		8000	proximal tibia

Table 7: Axial forces due to axial loading for 50% probability of calcaneus or tibia fracture

Study	Tibia axial force (N)		Measurement location
	Tibia fracture	Calcaneus fracture	
Begeman and Aekbote (1996)	8000		Proximal tibia
Kitagawa et al. (1998)	7239 (average measured)	8115 (average measured)	Proximal tibia
Klopp et al. (1997)	9300		Contact
McKay and Bir (2009)	5931		Mid tibia (implanted)
Schueler et al. (1995)	15,000 *		Sole
Yoganandan et al. (1999)		6200	Proximal tibia

*determined using relative risk

IV. STATEMENT OF PURPOSE

In studying foot and ankle trauma, the dynamic response of the complex prior to injury is of interest. To more fully characterize the response of the foot and ankle, the current study analyzed biofidelity to create response corridors and injury data to develop injury criteria.

It was hypothesized that impacts with the same energy input would yield similar responses, while impacts with the same velocity but different impactor masses would yield a more varied response. Thus, it was expected that energy would better characterize the response of the PMHS foot and ankle.

It was also hypothesized that initial position of the foot and ankle would affect the resulting response. It was expected that the axial forces would be less for a dorsiflexed foot compared to a neutral foot because the axis of the lower limb would not be aligned with the impactor's axis. Because of the off-axis loading, it was expected flexion moments would be higher in the presence of initial dorsiflexion, resulting in malleolar fractures characteristic of rotational loading. The off-axis loading could also lead to different injury criteria based on initial position.

Characterizing the response of the foot and ankle PMHS to a variety of initial conditions can aid the effort to reduce the risk of foot and ankle injuries to military personnel by providing data for use in designing a manikin suitable to studying simulated under-vehicle blast events. These data can be used to design a surrogate that more accurately mimics human response.

V. MATERIALS AND METHODS

A. EXPERIMENTAL SET-UP

The intruding floorpan after an under-vehicle landmine blast was modeled by a lightweight pendulum impacting the plantar surface of a lower limb PMHS. According to a protocol approved by the Medical College of Wisconsin, 15 lower limb PMHS were obtained from nine individuals. Each specimen was disarticulated at the knee. The proximal 10 cm of the tibia was denuded and had a Steinmann pin passed transversely through it to aid rigid fixation to the polymethylmethacrylate (PMMA). A pin was also placed at the insertion of the posterior cruciate ligament (PCL). No fractures were expected at the proximal tibia. During the potting procedure, the leg was aligned in the sagittal plane by maintaining the line from the midpoint of the lateral and medial malleoli to the PCL pin vertical. In the coronal plane, the leg was aligned by maintaining the line from the outermost aspect of the lateral malleolus to the PCL pin vertical.

A six-axis load cell (Denton Inc., Rochester Hills, MI) was placed at the proximal tibia with its center aligned with the pin at the PCL. Ballast mass was added behind the load cell to simulate the thigh mass. The amount of ballast mass was dependent on the mass necessary to yield a mass of 11.5 kg for the PMMA, load cell, instrumentation, and ballast mass. The lower leg mass of the 50th percentile male HybridIII manikin is 11.5 kg. This set-up is shown in Figure 4.

Each specimen was also instrumented with strain gages (Omega Engineering, Stamford, CT), acoustic emission (AE) sensors (Physical Acoustics Corporation, Princeton Jct., NJ), and reflective markers on the proximal tibia, medial malleolus, lateral

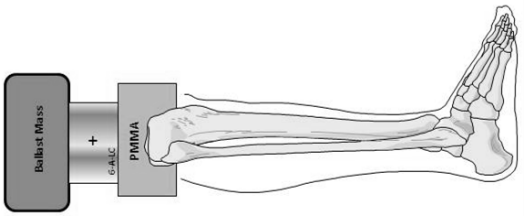

Figure 4: Lower limb PMHS preparation

malleolus, and calcaneus, as shown in Figure 5. Soft tissue was removed to expose the bone and allow direct attachment of the strain gages and AE sensors. For eight specimens the proximal tibia AE sensor was moved to the posterior calcaneus to be closer to the injury site. The last four specimens were not instrumented with AE sensors because the impact often caused them to debond from the bone. Since fracture was not expected at the proximal tibia or second metatarsal, small screws were inserted to mount reflective markers. Reflective markers were also adhered to the outer surface of the AE sensors on the medial side of the specimen.

The leg assembly was suspended from an overhead gantry by four lengths of lightweight steel cable (0.19 g/in), allowing the specimen to have initial flexion and to

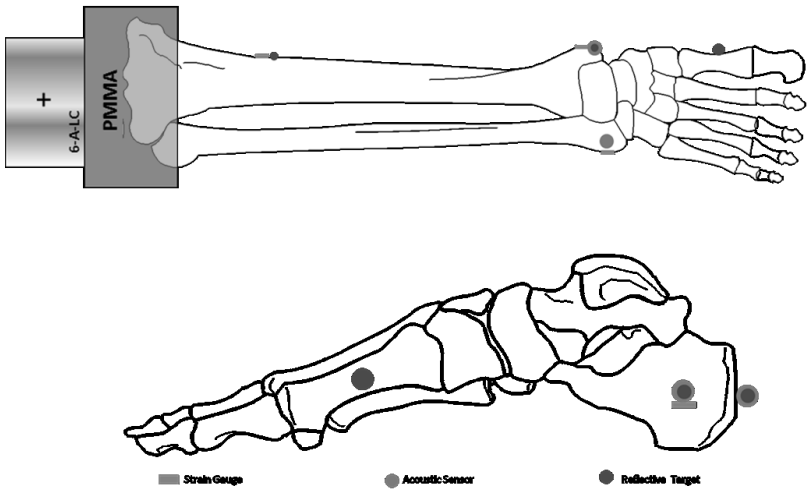

Figure 5: Anterior (top) and medial (bottom) views of instrumentation locations

translate after impact. At the proximal end of the assembly the cables attached to the metal plate used as ballast mass, while on the distal end the cables attached to a nylon strap around the ankle. The cable lengths could be changed to allow coarse adjustments to the height of the specimen above the ground as well as to the angle of the specimen's initial position. Turnbuckles inserted in the cables allowed fine adjustments to the position of the specimen. In contrast to other apparatuses, the adjustable cables allowed the ankle to be positioned in dorsiflexion with the plantar surface of the foot parallel to the impacting face of the pendulum. The support at the top of the gantry allowed right/left and forward/backward translation as well as rotation in the plane parallel to the floor to align the specimen with the center of gravity of the pendulum.

Each pendulum was instrumented with a uniaxial accelerometer (Endevco, San Juan Capistrano, CA) and a 4 in x 10 in x 0.5 in aluminum plate attached to the leading face for total masses of 3.3 kg, 5.7 kg, and 12.32 kg. The aluminum plate always engaged at least the heel and ball of the foot.

Neutral positioning, as shown in Figure 7, was defined in the sagittal plane by maintaining the line connecting the center of the load cell to the lateral malleolus horizontal. In the coronal plane, the line connecting the center of the load cell and the mid-point between the malleoli was perpendicular to the footplate on the pendulum. The height of the specimen above the ground was adjusted to align the pendulum’s center of gravity with the horizontal line in the sagittal plane, thereby directing the load along the tibial axis.

For initial dorsiflexion, the specimen was rotated 180-deg about the tibial axis, and the cables on the proximal end of the assembly were lengthened to lower the

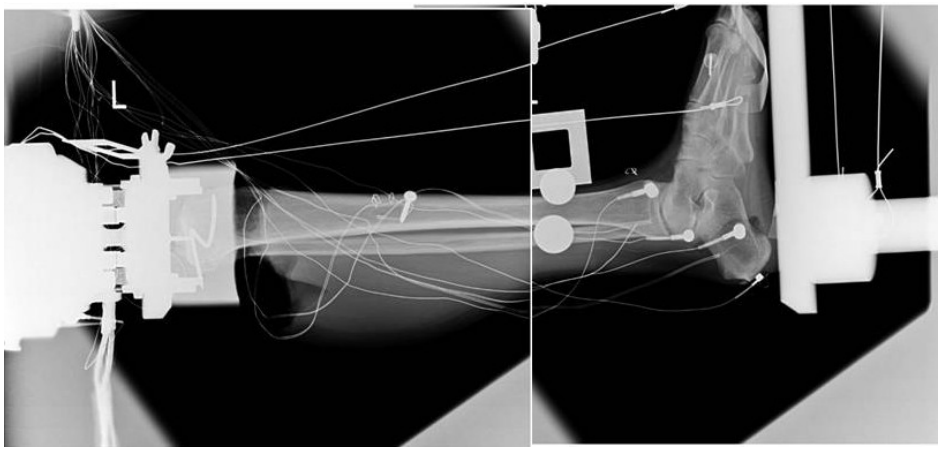

Figure 6: X-ray of initial alignment of pendulum, specimen, and load cell (Note: Images not to scale)

horizontal line in the sagittal plane 20-deg, as shown in Figure 7**.** Rotating the specimen 180-deg prevented tensioning of the cables at the ankle during impact. The pendulum's center of gravity was aligned with the lateral malleolus. Lateral x-rays were taken prior to the first test to verify instrumentation positioning and pendulum-specimen alignment (Figure 6**)**.

The foot was positioned with the plantar surface parallel to the impacting plate. A thin aluminum strip with steel cables attached to both ends was placed across the ball of the foot. The steel cables allowed adjustment to the position of the foot relative to the tibia and were attached to an aluminum plate between the PMMA and the load cell.

Impact velocities included 2-9 m/s, and thus impact energies included 7-500 J. An optical velocity gate measured pendulum velocity at impact. A rope was attached to the end of the ballast assembly and run through a pulley. Following impact, pulling on the rope increased the translation of the specimen. This mechanism prevented a second impact between the specimen and the pendulum.

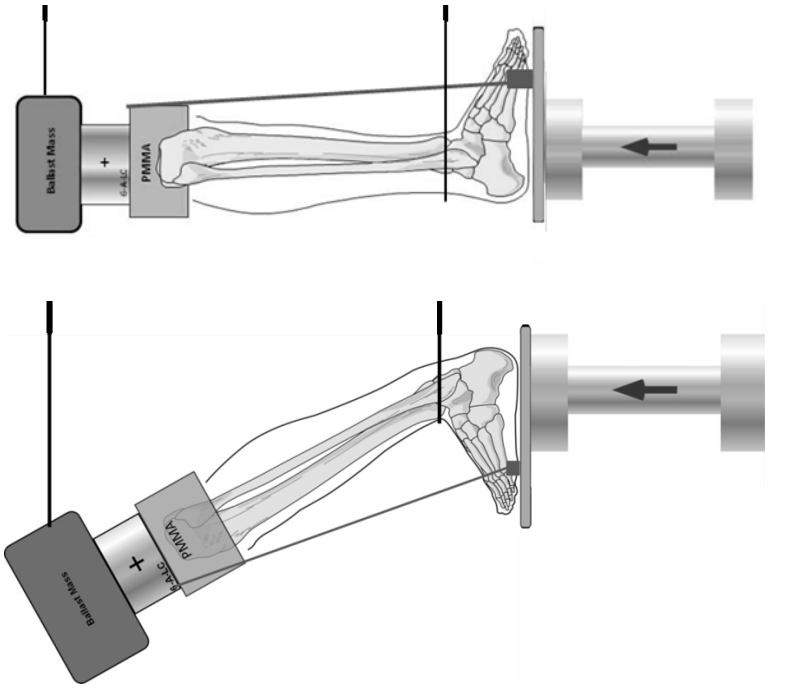

Figure 7: Neutral (top) and dorsiflexed (bottom) impact conditions

A test matrix was designed for each specimen using at least two of the three pendulums. Impact conditions were chosen such that identical energy and/or velocity levels were achieved by each pendulum. Each successive impact had a higher impact velocity and/or energy. A sample test matrix is shown in Table 10.

Four-six non-injury, or biofidelity, impacts were planned followed by an injury impact. Three specimens were repeatedly impacted at 5 m/s with the 3.30 kg pendulum to determine if significant changes in response occurred due to the multiple impacts. Tibia axial force and ankle compression were plotted to assess response.

A thin layer of conductive material was mounted to the plantar surface of the foot at the point of first contact with the pendulum to electronically trigger data collection and high-speed video recording, thereby establishing t = 0 s. Digital photographs of the assembly were taken before and after each test.

Table 8: Sample test matrix

Test Number	Pendulum Mass (kg)	Velocity (m/s)	Energy (J)
1	3.3	5	41.25
2	3.3	6	59.40
3	5.7	4.5	60.31
4	3.3	9	133.65
5	5.7	9	230.85

Strain gage, load cell, and accelerometer data were collected by a TDAS Pro System (DTS, Seal Beach, CA) at a sampling rate of 100,000 Hz. The amplifier of the data acquisition system had a roll-off frequency of 20,000 Hz and served as the anti-aliasing filter. AE data were recorded by a digital oscilloscope (Tektronix, Beaverton, OR) at a sampling rate of at least 1MHz. The AE sensors had an operating range of 150-400 kHz. High-speed video was collected at 1000 Hz, 3000 Hz, or 5000 Hz (DTI, Tallahassee, FL). Accelerometer, strain gage, and force data were filtered at CFC1000. Moment data were filtered at CFC600. AE data were filtered with a band-pass filter from 50k-400k Hz, according to the procedure introduced by Funk, Crandall et al. (2002).

After each impact, anterior/posterior and oblique calcaneus x-rays (MinXray, Northbrook, IL) were taken. Presence of injury was also assessed by palpation. Testing on the specimen ceased if clinically significant injury was observed. If no clinically significant injury was observed, the next impact in the test matrix was conducted following the same procedure. Once injury occurred, CT scans were obtained and an orthopaedic surgeon performed a dissection to visualize injury.

Intra-articular calcaneus fractures were classified by the clinically-developed Sander's scale (Khan et al., 2010). This classification system is based on a CT image in

the coronal plane with the widest view of the posterior facet (Khan et al., 2010). The type (I-IV) indicates into how many pieces the calcaneus is broken (Sanders & Clare, 2007). The letter (A-C) indicates the location of the primary fracture line in the posterior facet (Sanders & Clare, 2007). "A" corresponds to the lateral-most portion and "C" the medial-most portion (Khan et al., 2010).

B. BIOFIDELITY ANALYSIS

Force, moment, strain, and acoustic emission time histories were obtained for each specimen. Tibia axial force and ankle compression data from impacts to the same specimen with the same pendulum mass and impact velocity were compared to verify the validity of performing multiple non-injury impacts on one specimen.

Deflection, or ankle compression, was found from the high-speed video by calculating the change in distance between the pendulum and the medial malleolus markers during impact, as shown in Figure 8. Axial tibia force was then plotted against compression to obtain foot and ankle response. The resulting response curves had two distinct linear regions: heel pad response and ankle joint response. The stiffness in each region was found using linear regression as shown in Figure 9.

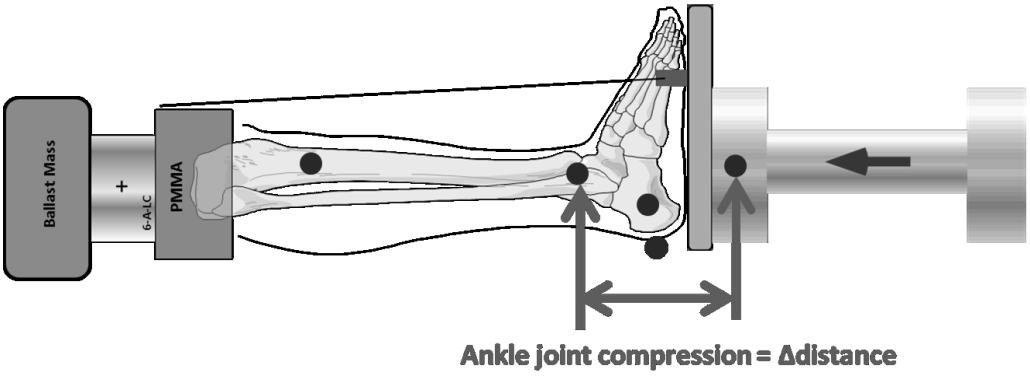

Figure 8: Ankle joint compression calculation from high-speed video using medial malleolus and pendulum markers

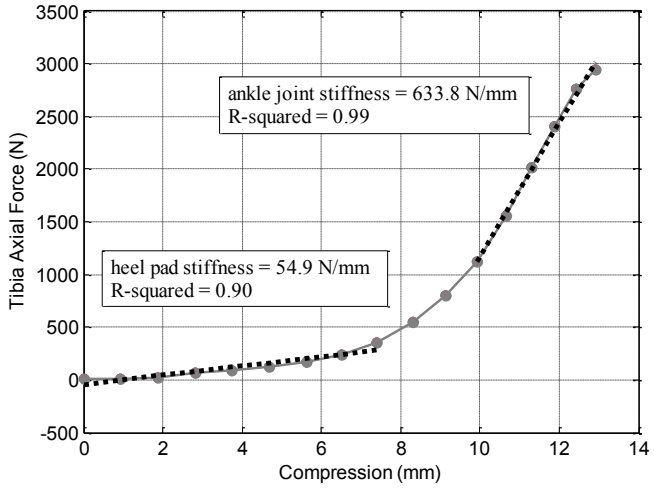

Figure 9: Sample calculation of heel pad and ankle joint stiffnesses using linear regression for a 4.9 m/s impact with the 3.3 kg pendulum (41 J)

Force-deflection plots from biofidelity impacts were separated based on initial position to develop response corridors. The two groups were then sub-divided by impact velocity and impact energy, resulting in four groups of data**.** Two-tailed t-tests were performed within the energy and velocity sub-groups using ankle joint and heel pad linear stiffness to identify low and high impact groups**.** Each group consisted of only one selected test per specimen.

A line with a slope of the average stiffness value defined the average response. Average ankle joint response initiated at the mean axial force of the first data points included in the linear regression for ankle joint stiffnesses of all tests included in the grouping. The initial compression value of the average response was determined by calculating the mean compression at the initial axial force value. Average ankle joint response terminated at the mean of the peak axial forces. Average heel pad response initiated at 0 mm of compression and the average of the axial forces at 0 mm. It terminated at the mean of the last axial force value included in the linear regressions in

the heel pad region. A corridor of 1σ was obtained using the standard deviation in axial force at 0 mm of compression and the standard deviation in compression at each force level of interest. The transition between heel pad and joint response at was not characterized. The corridors for energy were compared to those for velocity based on ankle joint stiffness to determine which better characterized the foot and ankle response.

Peak axial forces and flexion moments for impacts to neutral specimens were compared to those of dorsiflexed specimens using a two-tailed t-test for two independent samples. Data from impacts with 2 m/s, 3 m/s, 4 m/s, 26 J, and 100 J inputs were compared. Each group contained one selected test per specimen.

C. INJURY ANALYSIS

In developing injury risk curves, it is desirable to identify the axial force when fracture occurred. Force at fracture is considered an uncensored data point (Funk, Crandall et al., 2002). Injury could occur before the peak axial force is reached. In this case, peak axial force is not ideal for developing an injury risk curve. In the current study, axial force at fracture could be determined using strain or AE data. Thus, injury data points were considered uncensored. Logistic regression was performed using tests classified as biofidelity or injury to obtain injury risk curves applicable to neutral and dorsiflexed specimens. The fit of the regression was evaluated using log-likelihood ratio and chi-squared values.

VI. RESULTS

Table 9: Specimen information

Specimen Number L=Left/ R=Right	Test Numbers	Age (years)	Gender (F=Female /M=Male)	Height (m)	Total Body Mass (kg)
HS686L	PCLE200-206	47	M	1.78	80
HS686L	PCLE207-208	47	M	1.78	80
HS723R	PCLE215-219	56	F	1.70	79
HS731R	PCLE227-228	44	F	1.57	54
HS731L	PCLE229-230	44	F	1.57	54
HS658L	PCLE231-232	63	M	1.80	68
HS658R	PCLE233-237	63	M	1.80	68
HS643L	PCLE238-239	57	M	1.83	67
HS629R	PCLE240-242	58	M	1.79	75
HS730L	WC0101A001-002	49	M	1.83	86
HS730R	WC0101A003-004	49	M	1.83	86
HS735L	PCLE249-254	64	M	1.73	120
HS735R	PCLE255-261	64	M	1.73	120
HS734R	PCLE262-265	54	M	175	55
HS736L	PCLE266-268	57	M	1.80	89

Twelve male and three female specimens with an average age of 54 years were tested. Specimen information is detailed in Table 9. Each specimen was impacted 2-7 times. A total of 60 impacts were conducted. Nineteen impacts were to specimens in 20-deg of dorsiflexion and 41 to specimens in the neutral position. Thirty-five used the 3.30 kg pendulum, 16 the 5.70 kg, and 9 the 12.32 kg. Fifteen of the impacts to specimens in dorsiflexion and 25 impacts to specimens in neutral were non-injurious. The complete test matrix is in Table 10.

Table 10: Complete test matrix

Test Number	Pendulum Mass (kg)	Impact Velocity (m/s)	Impact Energy (J)	Initial Position*
PCLE200	3.30	2.02	6.76	N
PCLE201	3.30	3.99	26.22	N
PCLE202	5.70	3.04	26.40	N
PCLE203	5.70	4.02	46.14	N
PCLE204	5.70	5.95	100.75	N
PCLE205	3.30	7.71	97.96	N
PCLE206	5.70	9.05	233.22	N
PCLE207	3.30	2.07	7.07	N
PCLE208	3.30	2.01	6.69	DF
PCLE209	3.30	3.96	25.88	DF
PCLE210	5.70	3.03	26.17	DF
PCLE211	5.70	4.01	45.84	DF
PCLE212	5.70	5.93	100.29	DF
PCLE213	3.30	7.72	98.44	DF
PCLE214	5.70	8.97	229.55	DF
PCLE215	3.30	3.99	26.31	N
PCLE216	3.30	5.83	56.06	N
PCLE217	12.32	3.18	62.28	N
PCLE218	12.32	4.17	107.12	N
PCLE219	3.30	8.84	128.85	N
PCLE227	3.30	4.95	40.43	N
PCLE228	3.30	7.94	104.02	N
PCLE229	3.30	4.56	34.31	N
PCLE230	3.30	7.99	105.34	N
PCLE231	3.30	3.97	26.01	DF
PCLE232	3.30	7.93	103.76	DF
PCLE233	3.30	2.98	14.65	DF
PCLE234	3.30	6.75	75.18	DF
PCLE235	12.32	1.59	15.57	DF
PCLE236	12.32	3.64	81.62	DF
PCLE237	12.32	8.83	480.29	DF
PCLE238	3.38	3.99	26.92	DF
PCLE239	3.38	5.91	58.95	DF
PCLE240	3.38	3.05	15.70	DF
PCLE241	12.32	2.07	26.33	DF
PCLE242	12.32	3.06	57.85	DF
PCLE249	3.36	4.88	39.95	N
PCLE250	3.36	5.67	53.99	N
PCLE251	5.76	4.65	62.26	N
PCLE252	3.36	4.88	39.94	N
PCLE253	3.36	8.99	135.72	N
PCLE254	5.76	9.09	237.89	N
PCLE255	3.36	4.93	40.78	N
PCLE256	3.36	6.01	60.58	N
PCLE257	5.76	4.43	56.54	N
PCLE258	3.36	4.94	41.00	N
PCLE259	3.36	8.95	134.59	N
PCLE260	3.36	4.98	41.71	N
PCLE261	5.76	9.06	236.31	N
PCLE262	3.36	4.95	41.08	N
PCLE263	3.36	5.75	55.47	N
PCLE264	5.76	4.67	62.84	N
PCLE265	3.36	4.94	40.93	N
PCLE266	3.36	4.97	41.45	N
PCLE267	3.36	5.93	59.24	N
PCLE268	5.76	4.45	57.05	N
WC0101A001	12.32	3.20	63.05	N
WC0101A002	12.32	4.09	103.05	N
WC0101A003	5.70	4.43	56.04	N
WC0101A004	5.70	5.85	97.64	N

*DF=20-deg of dorsiflexion; N=neutral

The impacts were separated by initial position and then plotted as pendulum mass vs. impact velocity and pendulum mass vs. impact energy, as shown in Figure 10. Minor injuries to the neutral specimens indicated initiation of injury occurred at 4-5 m/s of 60 J.

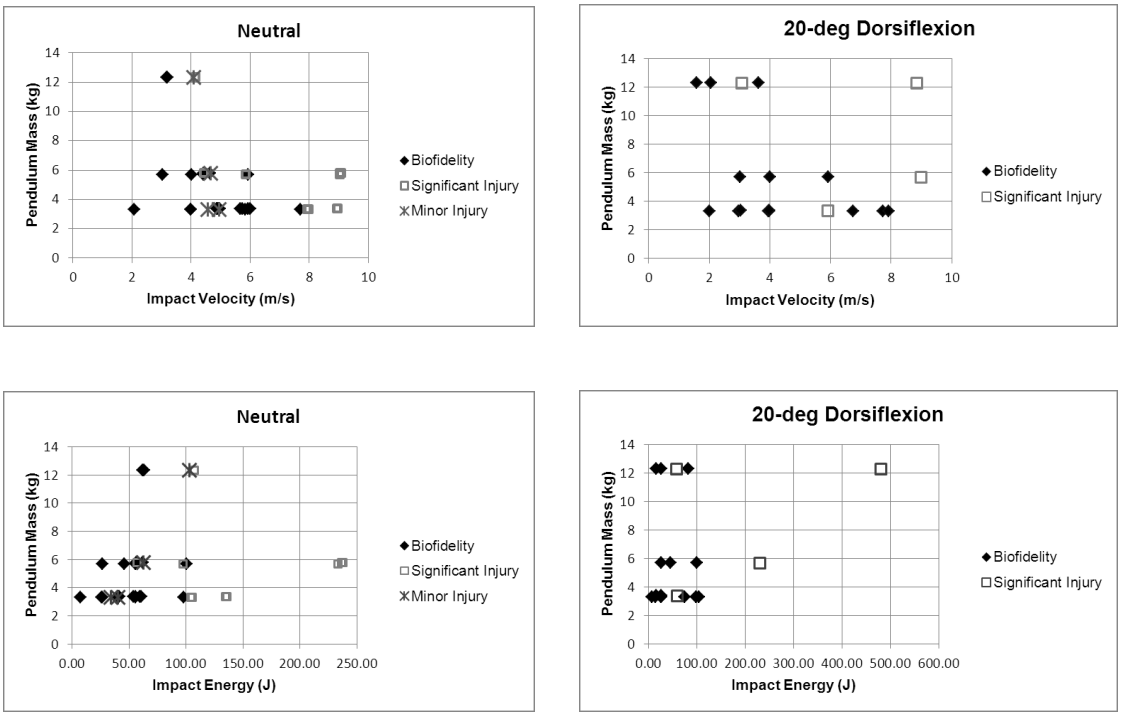

Figure 10: All pendulum impacts for neutral (left) and dorsiflexion (right) positioning based on pendulum mass and impact velocity or impact energy

Significant injuries began to occur at 100 J for neutral and 60 J for dorsiflexed specimens. The highest biofidelity, or non-failure, impacts occurred with the 3.3 kg pendulum at 8 m/s, resulting in an impact of 100 J.

Impacts were also plotted based on initial position as impact velocity or impact energy vs. peak tibia axial force, as shown in Figure 11. Overall, the peak tibia axial force increased with increasing velocity and energy. Non-injury impacts resulted in forces up to 8000 N for both initial positions. The lowest injury force for neutral specimens was 5000 N. The lowest for initially dorsiflexed specimens was 3800 N. Data from neutral specimens show minor injuries occurred at 3000-6000 N.

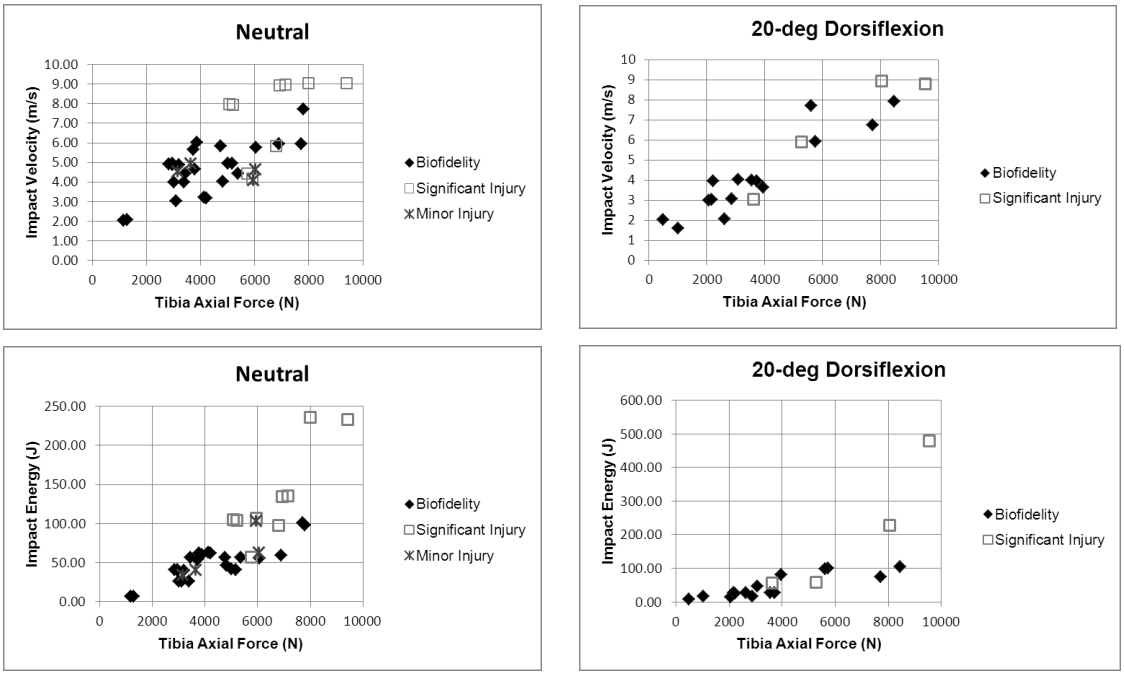

Figure 11: All pendulum impacts for neutral (left) and dorsiflexion (right) positioning based on impact velocity or impact energy and peak tibia axial force

A. BIOFIDELITY ANALYSIS

The data from all impacts to HS735L and HS735R are shown in Figure 12 and Figure 13**.** (Refer to results in VI.B: Injury Analysis for explanation of multiple injury impacts). In general, peak force and compression values increased with increasing impact velocity and energy. Peak forces from 5 m/s impacts with the 3.3 kg pendulum prior to injury are within 10% for both specimens. For HS735L, the compression values are within 2%, but for HS735R the pre-injury impacts (PCLE255 and PCLE258) are within 23%. However, the 3.3 kg pendulum impact at 5 m/s after the first injury impact (PCLE260) is within 0.06% of the peak compression in PCLE258. The third specimen with repeated 5 m/s impacts with the 3.3 kg pendulum was not included in this comparison because it did not have two of these impacts prior to injury.

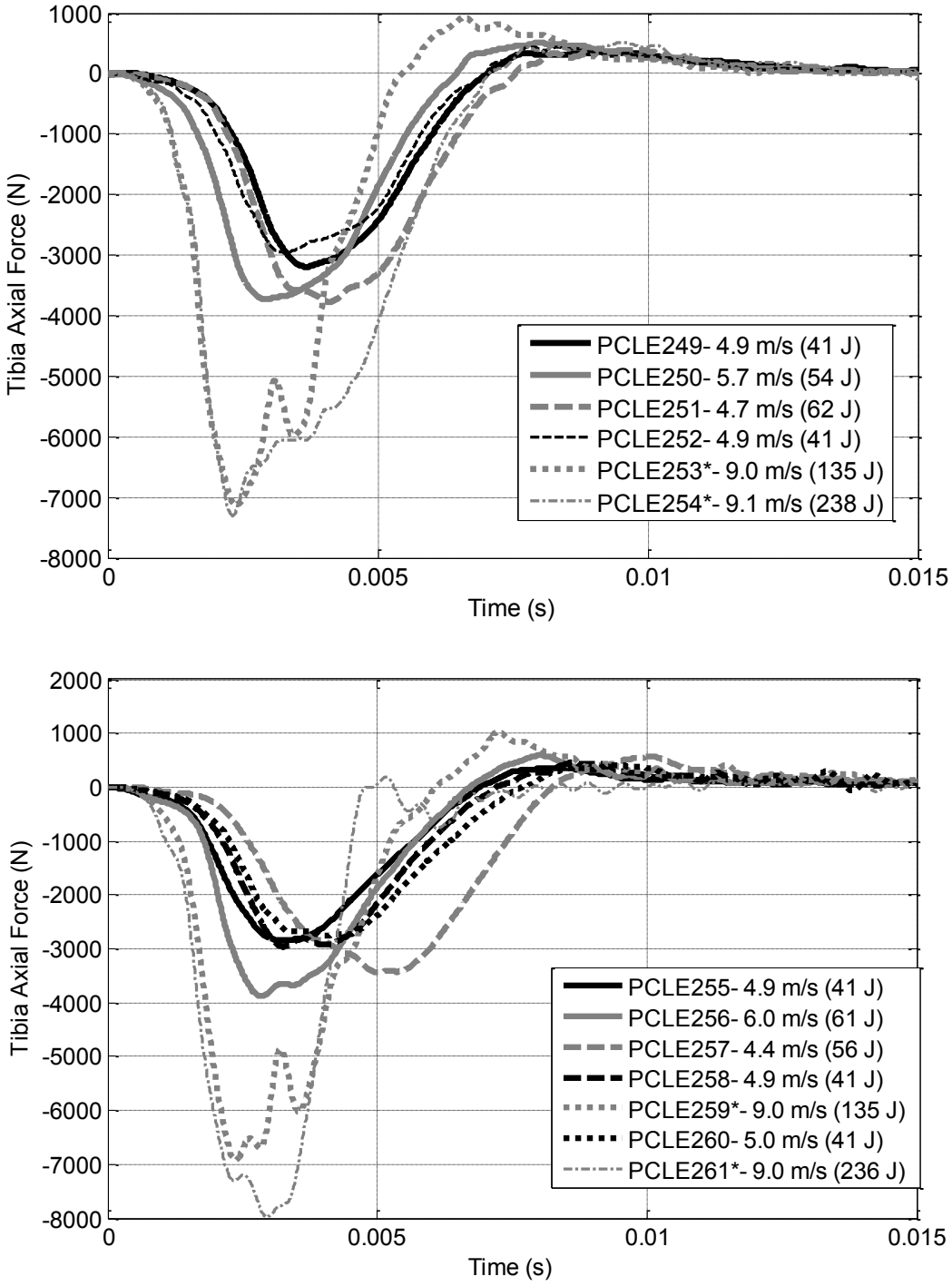

*Figure 12: Tibia axial force data for all impacts to HS735L (top) and HS735R (bottom). Black indicates a 5 m/s impact with the 3.3 kg pendulum, and * indicates injury impact*

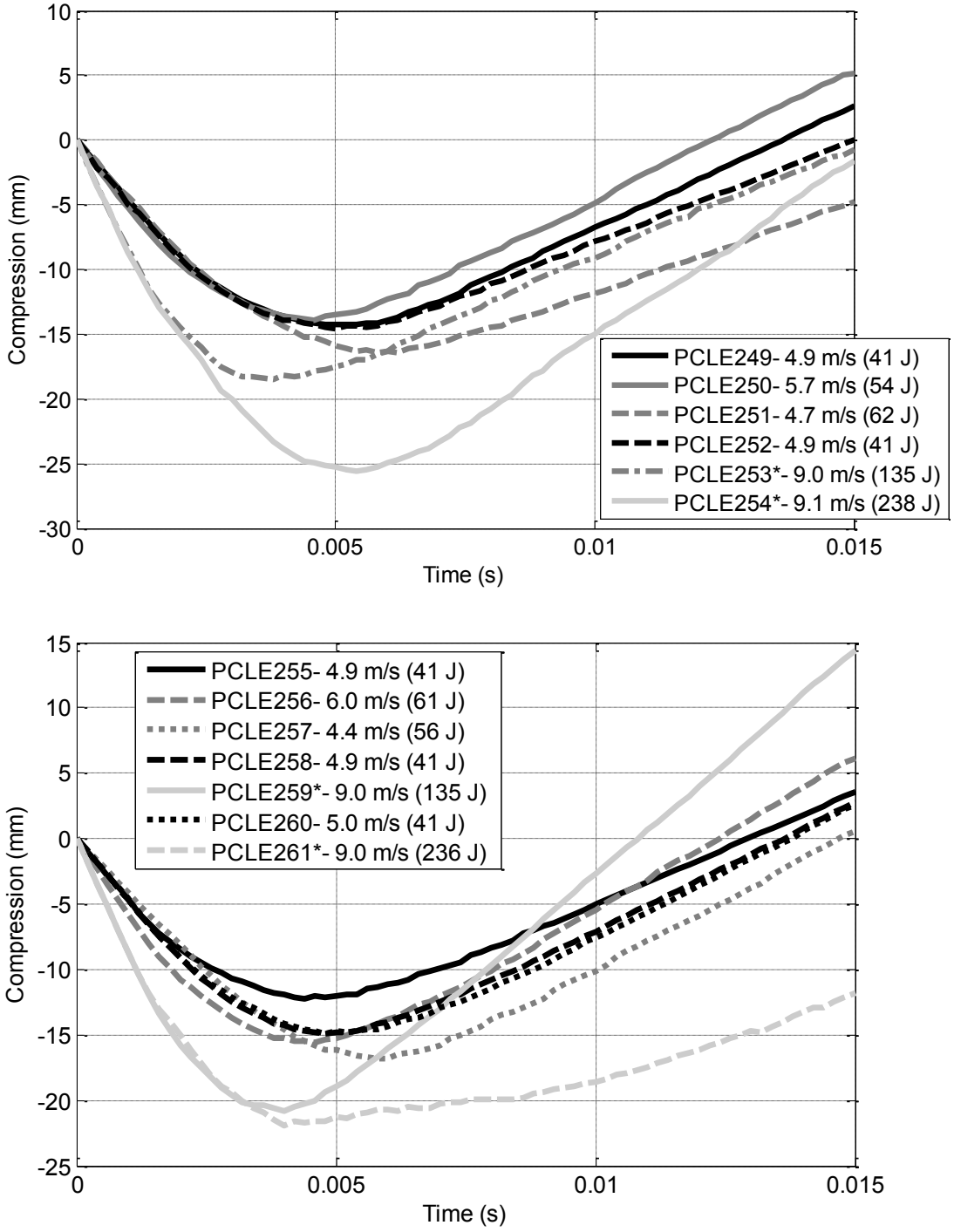

*Figure 13: Ankle compression data for all impacts to HS735L (top) and HS735R (bottom). Black indicates a 5 m/s impact with the 3.3 kg pendulum, and * indicates injury impact*

Table 11: Stiffness values for all impacts to HS735L and HS735R

HS735L			HS735R		
Test ID (*=injury **Bold** = same impact conditions)	Heel Pad Stiffness (N/mm)	Ankle Joint Stiffness (N/mm)	Test ID (*=injury **Bold** = same impact conditions)	Heel Pad Stiffness (N/mm)	Ankle Joint Stiffness (N/mm)
PCLE249	75.0	786.8	**PCLE255**	63.0	653.4
PCLE250	99.1	770.6	PCLE256	84.0	849.3
PCLE251	78.1	538.3	PCLE257	40.5	404.0
PCLE252	73.0	601.9	**PCLE258**	54.9	633.8
PCLE253*	109.0	1252.7	PCLE259*	143.4	1083.4
PCLE254*	88.4	1033.4	**PCLE260**	49.6	429.4
			PCLE261*	208.4	712.3

Heel pad and ankle joint stiffnesses for these impacts are given in Table 11. Similar to peak force and compression, stiffness values tended to increase when impact velocity and energy increased. For both HS735L and HS735R, heel pad and ankle joint stiffnesses for 5.5 m/s impacts with the 3.3 kg pendulum decreased as the number of impacts to the specimen increased. From PCLE249 to PCLE252, heel pad stiffness decreased by 0.3%, and ankle joint stiffness decreased by 24%. From PCLE255 to PCLE258, heel pad stiffness decreased by 13%, and ankle joint stiffness decreased by 3%. From the pre-injury impact (PCLE258) to the post-injury impact (PCLE260), heel pad stiffness decreased by 10%, and ankle joint stiffness decreased by 47%. Despite these decreases, higher stiffness values were found for injury impacts.

To determine the regions of heel pad response and ankle joint response, different thresholds for R^2 were used. The linear regression for heel pad response included the maximum number of consecutive data points starting from 0 mm of compression that yielded $R^2 \geq 0.90$. For joint response, the linear regression started at the data point of maximum axial force. Data points immediately prior were added one by one to the regression. In the region of ankle joint response, R^2 exhibited small fluctuations as data

points were added. When the linear regression included data points in the transition from heel pad response to ankle joint response, R^2 decreased with each additional data point. The ankle joint stiffness was taken from the last regression before the R^2 value started to decrease continually with added data points.

ANOVA was performed based on impact energy and velocity to see if three groupings could be created to develop corridors for each initial position. In neutral, all combinations of 2, 3, 4, 5, 5.75, 6 m/s and 7, 26, 40, 55, 63 J were tested. For initial dorsiflexion, all combinations of 1, 2, 3, 4, 5.75, 8 m/s and 6, 15, 26, 45, 75, 100 J were tested. When the ANOVA model was significant ($p<0.05$), a multiple comparisons test showed only two of the three groups had a significant difference. Thus, two-sample t-tests were used to identify groupings for impact energy and impact velocity by initial position.

The ankle joint stiffness of neutral specimens impacted at 2-3 m/s was significantly lower ($p < 0.05$) than the stiffness of specimens impacted at 4-6 m/s. The heel pad stiffness of these groups was not significantly different ($p > 0.05$). No significant difference in ankle joint or heel pad stiffness was found for energy groupings ($p > 0.05$). Groupings tested included: 7-26 J and 40-100 J; 7-26 J and 56-63 J; 7-40 J and 56-100 J; 7-56 J and 63-100 J; and 7 J and 26-100 J. There is a significant difference ($p < 0.05$) between the ankle joint stiffness at 4-6 m/s and at 7-63 J in neutral. One corridor was obtained for heel pad stiffness of neutral specimens. Three corridors were obtained for ankle joint stiffness and are shown in Figure 14.

The ankle joint stiffness of dorsiflexed specimens impacted at 1-3 m/s was significantly lower ($p < 0.05$) than the stiffness of specimens impacted at 6-8 m/s. The

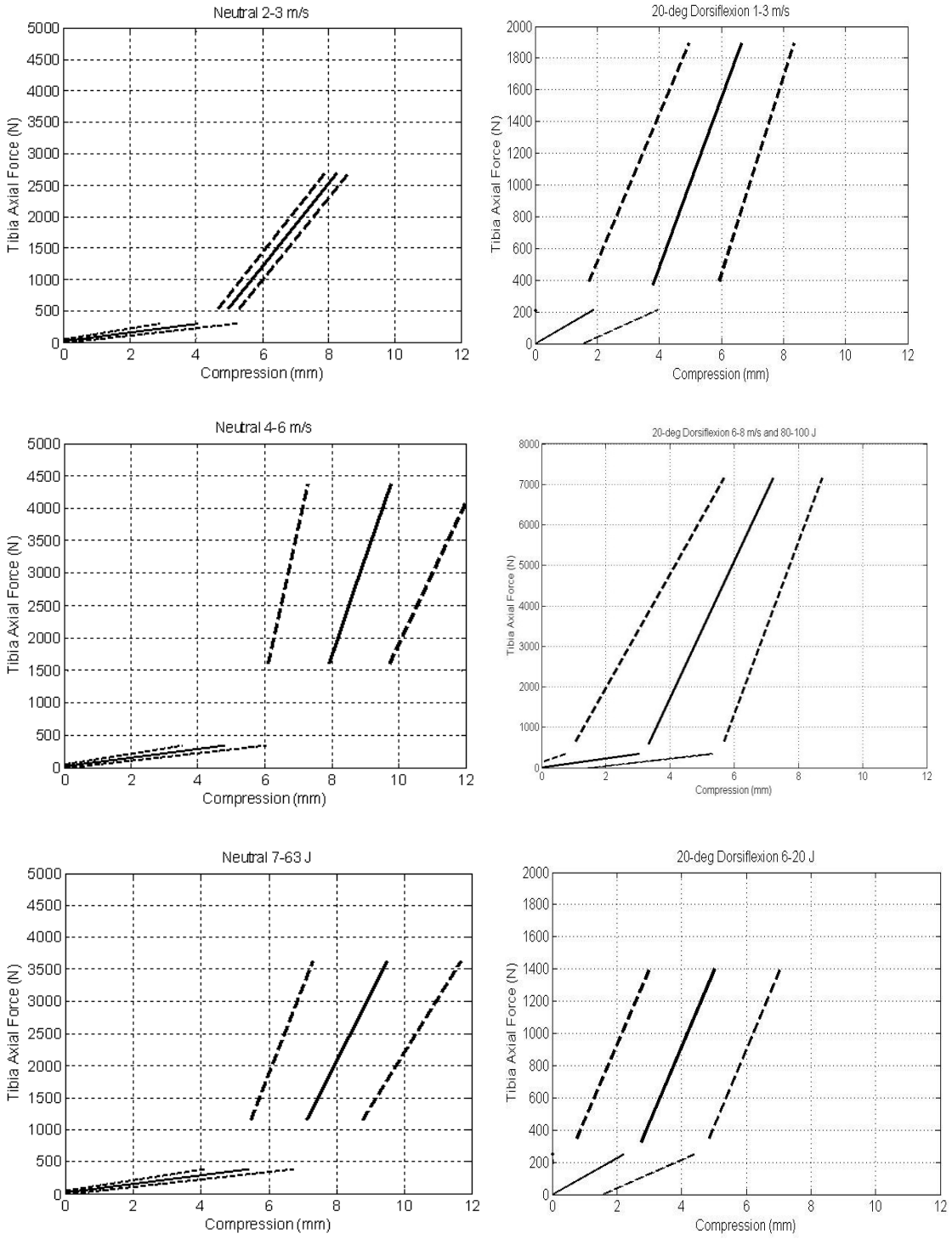

Figure 14: Velocity and energy corridors for neutral (left) and dorsiflexed (right) specimens

heel pad stiffness of these groups was not significantly different ($p > 0.05$). The joint stiffness of 7-20 J impacts was significantly different from 80-100 J ($p < 0.05$). Heel pad stiffness was not significantly different ($p > 0.05$). One corridor was obtained for heel pad stiffness of dorsiflexed specimens. Four corridors were obtained for ankle joint stiffness, but the 6-8 m/s and 80-100 J corridors were based on the same tests. While force and deflection values vary, no significant difference in ankle joint stiffness for 6-20 J and 1-3 m/s exists. In some tests with initial dorsiflexion the pendulum first contacted the ball of the foot instead of the heel. Since 0 mm of compression was chosen as first heel contact, axial forces were greater than 0 N at 0 mm compression. The average heel pad response was forced to start at 0 N for the given corridors. Results are shown in Figure 14.

While force and deflection values vary by grouping, there is not a significant difference ($p > 0.05$) in ankle joint stiffness in low or high impact velocity groups when comparing energy to velocity for dorsiflexed and neutral specimens. Furthermore, no significant difference ($p > 0.05$) in heel pad stiffness was observed between dorsiflexed and neutral specimens.

Peak tibia axial forces measured for dorsiflexed specimens were significantly different ($p < 0.05$) from neutral only for 3 m/s impacts. No difference ($p > 0.05$) was observed for 2 m/s, 4 m/s, or 26 J. Dorsiflexion moments were significantly different ($p < 0.05$) for 4 m/s impacts. No difference ($p > 0.05$) was observed for 2 m/s, 3 m/s, or 26 J. When grouped by impact energy at 26 J, no difference in peak axial force or peak dorsiflexion moment was seen.

B. INJURY ANALYSIS

Of the fifteen PMHS lower limbs tested, fourteen sustained an injury. For neutral specimens, the lowest impact velocity resulting in injury was 4.2 m/s and lowest energy was 57 J. The highest impact velocity without injury was 7.7 m/s and highest impact energy was 100 J. For dorsiflexed specimens, the lowest injurious velocity was 3 m/s and the lowest energy was 58 J. The highest impact velocity without injury was 7.9 m/s and the highest energy was 105 J.

All fourteen sustained calcaneus fractures and two also sustained tibia plafond fractures. Cortical defects on the medial wall of the calcaneus were considered minor injuries and not clinically significant. Three specimens sustaining a cortical wall defect were re-tested. In two specimens with a cortical wall defect, a more significant injury was suspected based on x-ray images; however, dissection revealed only the cortical wall defect. Four of the calcaneus fractures were intra-articular and involved the posterior facet, which articulates with the talus. Intra-articular fractures observed consistently had two calcaneal fragments broken at the medial zone of the posterior facet (Sanders II-B). All intra-articular fractures and cortical wall defects were observed in specimens positioned in neutral. Seven of the calcaneus fractures involved the posterior tuberosity.

All injuries are described in Table 12. After PCLE218, a fracture was identified in the x-ray images, but it was thought to be clinically insignificant. X-ray images showed the fracture of the calcaneus became more severe after PCLE219. Dissection showed the injury to be clinically significant. Thus, PCLE218 was chosen as the injury impact. Based on available x-ray images, an injury was suspected in HS658L after PCLE232, so no subsequent impacts were conducted. However, no injury was seen in

Table 12: Injury descriptions

Specimen ID	Test Number	Initial Position	Injury Location	Injury Description
HS686R	PCLE206	N	Calcaneus	joint depressed extending to sustentaculum tali and posterior facet (Sanders II-B)
HS686L	PCLE214	DF	Calcaneus	non-displaced on medial wall with incomplete extension into the sustentaculum tali, chondral fracture on medial aspect of posterior facet, and impaction of inferior aspect of posterior tuberosity
HS730L	WC0101A002	N	Calcaneus	cortical defect on medial wall
HS730R	WC0101A003	N	Calcaneus	cortical defect on medial wall
	WC0101A004		Calcaneus	posterior medial surface
HS723R	PCLE218	N	Calcaneus	plantar surface with some comminution
	PCLE219			
HS731R	PCLE227	N	Calcaneus	cortical defect on medial wall
	PCLE228		Calcaneus	posterior facet extending to posterior tuberosity (Sanders II-B)
HS731L	PCLE229	N	Calcaneus	cortical defect on medial wall
	PCLE230		Calcaneus	posterior facet extending to posterior tuberosity (Sanders II-B)
HS658R	PCLE237	DF	Calcaneus	inferior aspect of posterior tuberosity with some displacement
HS643L	PCLE239	DF	Calcaneus	non-displaced posterior inferior aspect of medial wall
HS629R	PCLE242	DF	Calcaneus	inferior aspect of medial wall
HS735L	PCLE253	N	Tibia	tibia plafond, along shaft in coronal plane
	PCLE254		Calcaneus	non-displaced inferior aspect of posterior tuberosity
HS735R	PCLE259	N	Tibia	tibia plafond, along shaft in coronal plane
	PCLE261		Calcaneus	posterior facet extending to posterior tuberosity (Sanders II-B)
HS734R	PCLE264	N	Calcaneus	cortical defect on medial wall
HS736L	PCLE268	N	Calcaneus	inferior aspect of posterior tuberosity with some displacement

the CT images or dissection. Therefore, PCLE231 and PCLE232 were considered non-injury.

The tibia fractures in HS735L and HS735R were not identified until post-test CT imaging and dissection were completed. The injuries were identified after PCLE253 and PCLE259 with calcaneus strain data. Data from subsequent impacts were not included in analysis, including the calcaneus fractures in PCLE254 and PCLE261.

CT and x-ray images of the calcaneus fractures in HS731L are shown in Figure 15 and Figure 16. After the first impact, only a cortical defect on the medial calcaneal wall was observed near the mounting site of the strain gage and AE sensors. Since a cortical

Figure 15: CT image (top-left) and x-ray images (top-right and bottom) of intra-articular calcaneus fracture in HS731L after PCLE230. Two other specimens sustained a similar fracture

defect is not a clinically significant injury, the next impact in the test matrix was performed. This impact resulted in the intra-articular fracture shown in Figure 15. The cortical defect did not coincide with the intra-articular fracture path. Two other specimens were impacted again after a cortical defect was observed on the medial calcaneus. The most severe injury to HS730L and HS734R was a cortical defect on the calcaneus.

Figure 16: X-ray image of cortical defect on medial wall in HS731L after PCLE229. Four other specimens sustained a similar clinically insignificant injury

To obtain uncensored force data, strain and AE data were used to identify time of injury. Since injury primarily occurred at the calcaneus, data from calcaneus strain gages and acoustic emission sensors were used. However, due to the irregular shape of the calcaneus and the size of the sensor, the acoustic emission sensors debonded during injury impacts in six of the first ten specimens tested. In contrast, strain gages debonded in three of the first ten injury tests. Strain data were available until the time of peak force in two of the impacts.

A burst of acoustic emission, where the measured voltage exceeded the baseline noise, indicated failure (Figure 17). In five of the first ten impacts where a clinically

significant injury was observed in the imaging and dissection, the acoustic emission from the fractured bone showed no change from the baseline signal (Figure 18). Significant changes in acoustic emission were seen in sensors attached to the lateral malleolus in two of the first ten specimens (Figure 18). The sensor debonded during one of these two impacts. No fracture was evident in the lateral malleolus.

The morphology of the calcaneus strain curve was observed to have the same characteristics as the axial force curve in non-injury impacts and prior to injury in injury impacts (Figure 19). In non-injury impacts, the calcaneus strain and tibia axial force curves had the same morphology for the entire data set. In injury impacts, a deviation of the calcaneus strain from the tibia axial force indicated injury. Thus, time of injury was identified by the deviation of the curves, as shown in Figure 19. The axial force at that time was chosen as the failure force. If no deviation occurred before peak axial force, the peak force was used as force at fracture.

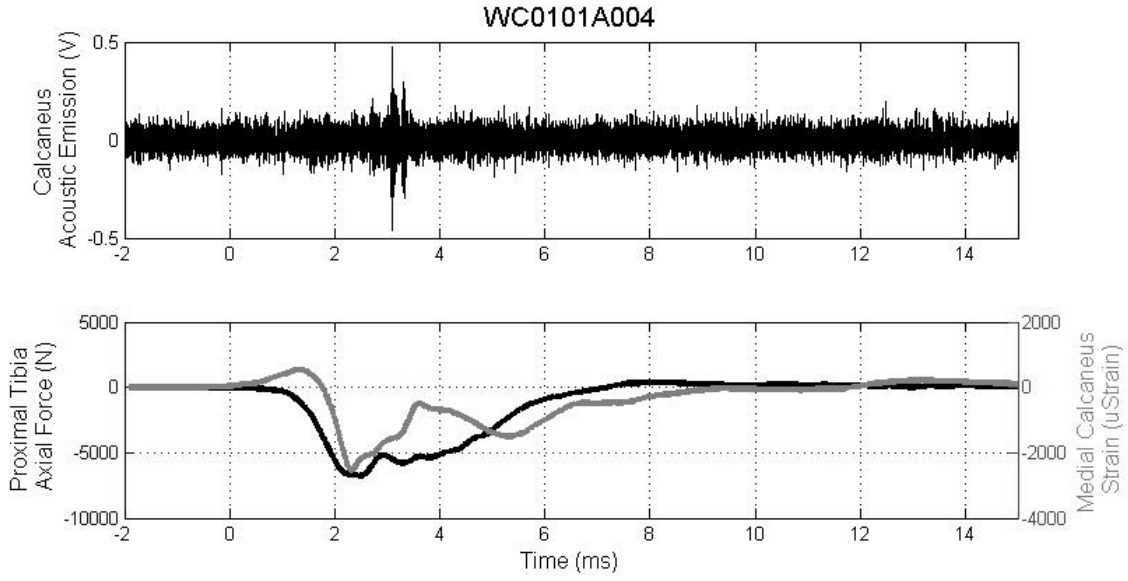

Figure 17: Identification of known injury by calcaneus acoustic emission sensor (top) and calcaneus strain gage (bottom)

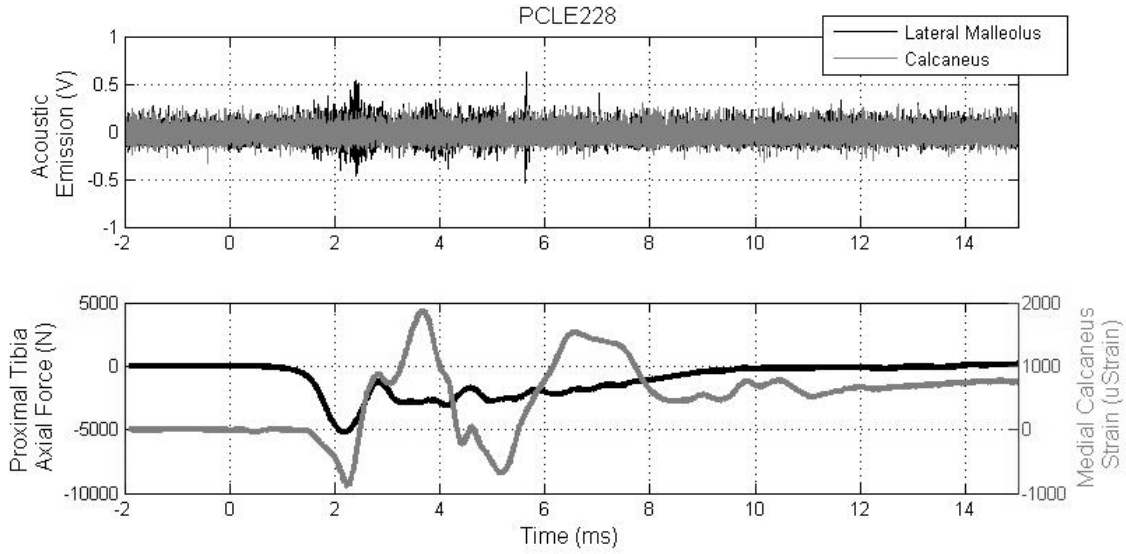

Figure 18: Identification of known injury by calcaneus strain gage (bottom) and lateral malleolus acoustic emission sensor (top) but not calcaneus acoustic emission sensor (top)

For the eight clinically significant injuries produced in neutral specimens, fracture force was identified as peak axial force in three cases. The other five injury tests yielded forces at fracture 2-16% smaller than the peak axial force. Logistic regression using uncensored data from 32 neutral tests yielded a log-likelihood ratio of -14.2 and a chi-squared value of 7.7 ($p = 0.0057$). Tibia axial force of 6800 N corresponded to 50% probability of injury in neutral.

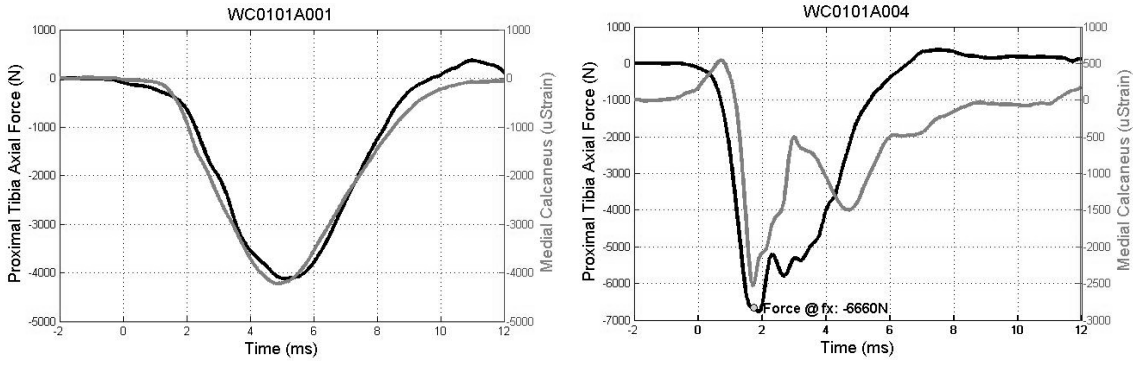

Figure 19: Comparison of calcaneus strain and tibia axial force data for a non-injury (left) and injury (right) impact

Of the four injury tests for dorsiflexed specimens, three had peak axial force as force at fracture. The fourth injury test had a force at fracture 19% lower than the peak force. Logistic regression using uncensored data from 19 dorsiflexion tests yielded a log-likelihood ratio of -8.1 and a chi-squared value of 3.4 ($p = 0.067$). In dorsiflexion, 50% probability of injury occurs at 7900 N, but this result was not statistically significant.

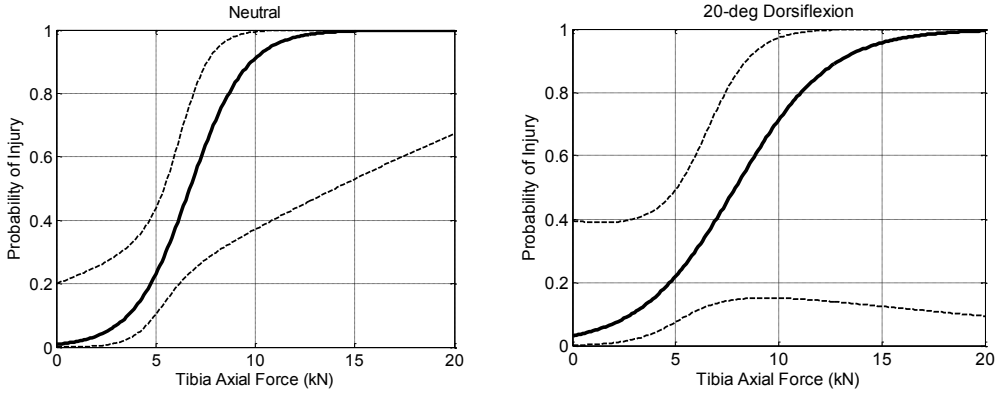

Figure 20: Injury risk curves for neutral (left) and dorsiflexed (right) specimens with 95% confidence intervals

VII. DISCUSSION

Non-injury and injury data obtained from 60 pendulum impacts to 15 PMHS lower limb specimens were analyzed to characterize foot and ankle response based on initial position as well as impact velocity and energy.

The validity of performing multiple non-injury impacts on one specimen was evaluated by comparing tibia axial force, ankle compression, and stiffness values from the same specimen for identical impact conditions. Results from identical impacts on HS735R and HS735L showed some variation in response is present. Tibia axial force was the most consistent measure. The change in compression between repeated impacts prior to injury was small for HS735L but large for HS735R. While heel pad and ankle joint stiffnesses from identical impacts decreased as more impacts were conducted, differences ranged from 0.3-23%. These mixed results indicate some variation in response due to multiple impacts is present; however, that variation may be small. Furthermore, degree of variation may vary from specimen to specimen.

By performing multiple non-injury impacts on each specimen, more data were obtained using fewer specimens. The current study used data from 52 impacts to 15 specimens. Data were available on response to low impacts and high impacts for each specimen. Manning et al. (1997) similarly applied dorsiflexion loading to five PMHS lower limbs 28 times at sub-injury levels. However, they did not investigate any changes in response due to the multiple impacts. In contrast, Funk, Crandall et al. obtained 43 specimens to perform 43 tests, generating mostly injury data (2002). In the existing literature for axial loading at most two impacts per specimen were performed. The second impact was conducted because the expected injury did not occur after the first

impact (Yoganandan et al., 1996). Performing multiple non-injury impacts per specimen greatly increases the data available for non-injurious biofidelity evaluations.

The axial compliance of the foot and ankle region prior to injury was characterized using heel pad and ankle joint stiffness. Stiffness values were obtained using axial force and compression data. While the corridors for energy and velocity groupings overlap, the ankle joint stiffnesses are significantly different.

For neutral specimens, the ankle joint stiffnesses became significantly different around 3-4 m/s. In contrast, for dorsiflexed specimens, large variations in stiffness were seen in the 4-5 m/s range. Thus, the velocity corridors for dorsiflexed specimens (1-3 m/s and 6-8 m/s) did not include a continuous range of velocities like the corridors for neutral specimens (2-3 m/s and 4-6 m/s).

Significant differences in stiffness were not seen for neutral specimens based on impact energy in this study. Dorsiflexed specimens were divided into two groups based on energy; however, the high-energy group consisted of the same tests included in the high velocity group. Furthermore, the corridors developed for the low energies and low velocities had substantial overlap and no significant difference in ankle joint stiffness ($p > 0.05$).

Foot and ankle response for this data set did not appear to be sensitive to impact energy for either neutral or dorsiflexed specimens. The response appears more sensitive to velocity but differs based on initial position. Due to limiting data in each group to one impact per specimen, sample sizes are small ($n<9$ in neutral and $n=3$ in dorsiflexion). Future test matrices will be designed to increase the data points available for each grouping.

Crandall et al. (1996) reported a maximum of 4 mm of compression for dynamic axial pendulum impacts at 5 m/s with an unspecified mass. This result was obtained by using tibia and floorplate accelerations to calculate compression (Crandall et al., 1996). Compression found using heel and distal tibia markers in high-speed video confirmed these values (Crandall et al., 1996). They did not differentiate heel pad compression from ankle joint compression (Crandall et al., 1996). The current study found 4 mm to be in the region of heel pad compression with ankle joint corridors terminating at 9-12 mm.

McKay reported axial force vs. intrusion corridors (2010). Unlike the previous results, he assumed the knee was fixed during the impact and used data from a laser transducer to measure footplate displacement. A constant force in the range of 0-700 N is seen until 5 mm of compression in the data presented by McKay (2010). This range is similar to the heel pad region of the current corridors but has a slope of 0 N/mm. A maximum force of 5500 N was reported at 25 mm of compression for 7 m/s impacts in McKay's study (2010). The 4-6 m/s corridor for neutral specimens in the current study reached a peak force of 4300 N at 9.5 mm compression. Compression values in the current study are different from those reported in the current literature. Differing definitions of "intrusion" and "compression" could contribute to the differing results. Unlike the other studies in the literature, the corridors in the current study compared foot and ankle response at low velocities to high velocities.

In the current study, differences in axial force and flexion moment between neutral and dorsiflexed specimens were only found at 3 m/s and 4 m/s respectively. No overall decrease in axial force or increase in flexion moment was seen for specimens with initial dorsiflexion. Only Klopp et al. (1997) provided force and moment values for

specimens axially loaded in neutral and in initial dorsiflexion. However, impact velocities were not provided, so the results are not analogous to the current study. The axial force measured in five neutral specimens was higher ($p < 0.05$) than in 11 specimens with 5-15-deg of dorsiflexion. There was no significant difference in flexion moment ($p > 0.05$). The difference in force may be due to different impact velocities for the two groups. Comparisons between initial positions were more informative in the current study because they were made based on impact velocity and energy. However, sample size was small (n=2-5).

When seen clinically, the non-displaced calcaneus fractures produced in this study would be treated non-surgically (Khan et al. 2010). However, the injured limb would need to be immobilized in a cast and elevated (Khan et al. 2010). The intra-articular fractures would be treated surgically (Khan et al. 2010). The surgery would aim to correct for any loss of calcaneal height and shortening/widening of the heel (Sanders & Clare, 2007). Widening of the heel can also trap tendons against the lateral malleolus (Sanders & Clare, 2007). These changes in the shape of the calcaneus alter subtalar motion (Sanders & Clare, 2007). Patients can be partially incapacitated for up to three years following injury (Sanders & Clare, 2007).

Similar to studies using axial loading in the literature, the current experimental series created mostly calcaneus fractures. The distribution of injuries was most similar to the injuries seen by Yoganandan et al. (1996): intra-articular and extra-articular calcaneus fractures with some distal tibia fractures. The experimental set-up used by Yoganandan et al. (1996, 1999) was the most similar to the current study because the proximal tibia

was not fixed, specimens were sectioned at the knee, no Achilles' tensioning or axial pre-loading was present, and ballast mass was added to the assembly.

All specimens placed in 20-deg of dorsiflexion sustained calcaneus fractures, which based on current literature are characteristic of axial loading. Of the five injured specimens with an initial position of 10-15-deg from the study by Klopp et al. (1997), three sustained a calcaneus fracture, one a talus fracture, and one sustained ligament tears. When specimens were axially loaded with initial dorsiflexion up to 20-deg, no malleolar fractures, which were the primary fracture mode under dynamic dorsiflexion loading, were observed in the current study or in the literature. Since Klopp et al. (1997) obtained initial dorsiflexion by rotating the footplate, the load was still directed along the tibial axis. In the current study, since dorsiflexion was obtained by changing the height of the proximal tibia, the load was not directed along the tibial axis. Despite this difference, neither set-up resulted in malleolar fractures.

In contrast, Funk et al. (2000) were able to create malleolar fractures, an injury characteristic of rotation, in specimens with 30-deg of initial plantarflexion, 10-deg of initial inversion, and neutral positioning. Funk et al. (2000) used the same experimental set-up as Klopp et al. (1997). However, in Funk et al.'s study (2000) 16 cm of intrusion was permitted. When the intrusion was reduced to 6 cm fewer malleolar fractures were observed (Funk et al., 2000). The level of intrusion may be a key component in creating rotational injuries under axial loading.

In current literature, tibia pylon fractures were only found under axial loading. The tibia plafond fractures found in the current study could be the beginning of a tibia pylon fracture. All studies creating tibia pylon fractures fixed the proximal tibia

(Begeman and Aekbote, 1996; Funk, Crandall et al., 2002; Kitagawa et al., 1998; McMaster et al., 2000). Furthermore, two investigators impacted the specimens anterior to the tibia axis (Begeman and Aekbote, 1996; Kitagawa et al., 1998). It is hypothesized that no tibia pylon fractures resulted in the current study because the impact was along the tibia axis and the proximal tibia was allowed to translate.

Klopp et al. (1997) postulated that specimens with initial dorsiflexion are less likely to be injured under similar conditions to neutrally positioned specimens because there is greater contact area between the talus and tibia/fibula when the foot is in dorsiflexion. In the current study two specimens with 20-deg of dorsiflexion were impacted at 8 m/s by a 3.3 kg pendulum and were uninjured. In contrast, three neutral specimens experienced the same impact and two were injured.

The lack of injuries in the current study that are characteristic of studies with dorsiflexion loading is supported by the measured flexion moments. Studies in literature propose 60 Nm and 85 Nm as flexion moments for a 50% probability of injury (Kuppa et al., 1997; Petit et al., 1996; Rudd et al., 2004). Only one of the four impacts to specimens with initial dorsiflexion that resulted in injury had a peak flexion moment greater than 60 Nm.

The current study is the first to compare the use of strain gages to acoustic emission sensors in identifying time of injury. Funk, Crandall et al. (2002) found no acoustic emission in specimens that did not fracture and found acoustic emission is specimens that did fracture. The current study had mixed results with AE sensors because they debonded during impact. Similar to McKay and Bir (2009), calcaneus

strain gages were used to identify time of injury. However, the current study could not assume injury occurred at peak axial force.

The injury risk curves for neutral and dorsiflexion impacts are similar. The 6800 N found for 50% probability of injury in neutral is most applicable to calcaneus fractures. This value is similar to the 6200 N reported by Yoganandan et al. (1999) for calcaneus fractures.

The injury risk curve obtained for dorsiflexion was not statistically significant ($p > 0.05$). Fewer data points were available for dorsiflexion than for neutral. The current value of 7900 N for 50% probability for injury is higher than the 6800 N for neutral specimens. This difference further supports Klopp et al.'s claim (1997) that the increased contact area at the subtalar joint due to dorsiflexion results in a lower risk of injury. The injury pattern observed indicates that despite initial dorsiflexion, no significant rotation occurs at the ankle. It is presumed that an improved injury risk curve could be obtained with additional impact tests with initial dorsiflexion.

The current study has several limitations. Compression values were calculated from high-speed video taken in the sagittal plane. While force data indicates off-axis loads were small compared to the axial load, no data is available to confirm the specimen translated purely in the sagittal plane after impact. Compression values could be affected by out-of-plane motion. Furthermore, it would have been ideal to calculate compression at the calcaneus, but the marker often debonded during impact.

The inconsistencies seen in the results of identical impacts to the same specimen indicate the results could be limited by using multiple impacts. Additionally, soft tissue was removed to expose the bone in order to mount instrumentation. The disruption of the

soft tissue and mounting of the instrumentation may have influenced the presence of minor injuries because cortical defects in the calcaneal wall occurred at the location of instrumentation.

When the specimen was positioned in dorsiflexion, the off-axis loading may have caused tensioning in the supporting cables at the ankle and ballast mass. Thus, forces and moments measured by the load cell at the proximal tibia may be compromised.

VIII. CONCLUSIONS

Corridors for biofidelic foot and ankle response were developed based on impact velocity and impact energy for lower limb PMHS initially in neutral and in 20-deg of dorsiflexion. Energy and velocity groupings were determined based on ankle joint stiffness. It was expected that energy would better characterize the response because it includes impact mass. However, only one corridor was obtained for energy in neutral. In dorsiflexion, the high energy corridor matched the high velocity one. Thus, foot and ankle response was not characterized by energy in this study. The velocities included in the low and high impact corridors differ by position: 2-3 m/s and 4-6 m/s in neutral, and 1-3 m/s and 6-8 m/s in dorsiflexion. The results of the current study indicate a lower limb surrogate should be sensitive to both heel pad stiffness and ankle joint stiffness.

Future testing will use the same apparatus to impact lower leg manikins. The response of the manikin will be compared to the response of the PMHS. Furthermore, a new apparatus will be designed to use higher velocity impacts with an even lower impactor mass to be more characteristic of the military environment.

It was expected that specimens in 20-deg of dorsiflexion would experience higher flexion moments and lower axial forces due to the off axis loading. A significant difference was not observed between the two positions. However, logistic regression yielded a smaller axial force for 50% probability of injury in neutral (6800 N) than in dorsiflexion (7900 N). The initial dorsiflexion did not induce the rotation or bending necessary to produce malleolar fractures previously found in dorsiflexion loading studies. Future tests will constrain the motion of the proximal tibia in an attempt to produce more severe injuries that have been reported in the military environment.

BIBLIOGRAPHY

Begeman, P. C., & Aekbote, K. (1996). Axial load strength and some ligament properties of the ankle joint. *6th Injury Prevention through Biomechanics Symposium,* Detroit, MI. 125-135.

Begeman, P. C., Balakrishnan, P., Levine, R., & King, A. I. (1993). Dynamic human ankle response to inversion and eversion. *37th Stapp Car Crash Conference,* San Antonio, TX. 83-93.

Begeman, P. C., & Prasad, P. (1990). Human ankle impact response in dorsiflexion. *34th Stapp Car Crash Conference,* Orlando, FL. 39-53.

Bellabarba, C., Barei, D. P., & Sanders, R. W. (2007). Dislocations of the foot. In M. J. Coughlin, R. A. Mann & C. L. Saltzman (Eds.), *Surgery of the foot and ankle* (8th ed., pp. 2137-2198). Philadelphia, PA: Mosby.

Bir, C., Barbir, A., Dosquet, F., Wilhelm, M., van der Horst, M., & Wolfe, G. (2008). Validation of lower limb surrogates as injury assessment tools in floor impacts due to anti-vehicular land mines. *Military Medicine, 173*(12), 1180-1184.

Bird, R. (2001). Protection of vehicles against landmines. *Journal of Battlefield Technology, 4*(1), 14-17.

Boon, A. J., Smith, J., Zobitz, M. E., & Amrami, K. M. (2001). Snowboarder's talus fracture. Mechanism of injury. *The American Journal of Sports Medicine, 29*(3), 333-338.

Carr, J. B., Hamilton, J. J., & Bear, L. S. (1989). Experimental intra-articular calcaneal fractures: Anatomic basis for a new classification. *Foot & Ankle, 10*(2), 81-87.

Crandall, J. R., Kuppa, S. M., Klopp, G. S., Hall, G. W., Pilkey, W. D., & Hurwitz, S. R. (1998). Injury mechanisms and criteria for the human foot and ankle under axial impacts to the foot. *International Journal of Crashworthiness, 3*(2), 147-162.

Crandall, J. R., Hall, G. W., Bass, C. R., Klopp, G. S., Hurwitz, S. R., Pilkey, W. D., . . . Lassau, J. P. (1996). Biomechanical response and physical properties of the leg, foot, and ankle. *40th Stapp Car Crash Conference,* Albuquerque, NM. 173-192.

Drake, R. L., Vogle, A. W., & Mitchell, A. W. M. (2010). Lower limb. In W. Schmitt, & R. Gruliow (Eds.), *Gray's anatomy for students* (2nd ed., pp. 510-647). Philadelphia, PA: Churchill Livingstone.

Funk, J. R. (2000). The effect of active muscle tension on the axial impact tolerance of the human foot and ankle complex. (Unpublished Biomedical Engineering PhD). University of Virginia.

Funk, J. R. (2011). Ankle injury mechanisms: Lessons learned from cadaveric studies. *Clinical Anatomy (New York, N.Y.), 24*(3), 350-361.

Funk, J. R., Crandall, J. R., Tourret, L. J., MacMahon, C. B., Bass, C. R., Patrie, J. T., . . . Eppinger, R. H. (2002). The axial injury tolerance of the human foot and ankle complex and the effect of achilles tension. *Journal of Biomechanical Engineering, 124*(6), 750-757.

Funk, J. R., Srinivasan, S. C. M., Crandall, J. R., Khaewpong, N., Eppinger, R. H., Jaffredo, A. S., . . . Petit, P. Y. (2002). The effects of axial preload and dorsiflexion on the tolerance of the ankle/subtalar joint to dynamic inversion and eversion. *46th Stapp Car Crash Conference,* Ponte Verdra Beach, FL.

Funk, J. R., Tourret, L. J., George, S. E., & Crandall, J. R. (2000). The role of axial loading in malleolar fractures. *SAE 2000 World Congress,* Detroit, MI, SAE 2000-01-0155

Geurts, J., van der Horst, M., Leerdam, P. J., Bir, C. A., van Dommelen, H., & Wismans, J. (2006). Occupant safety: Mine detonation under vehicles a numerical lower leg injury assessment. *2006 International IRCOBI Conference,* Madrid, Spain. 373-376.

Hirsch, C., & Lewis, J. (1965). Experimental ankle-joint fractures. *Acta Orthopaedica Scandinavica, 36*(4), 408-417.

Horst, M.J., Simms, C.K., Maasdam, R. & Leerdam, P.J.C. (2005). Occupant lower leg injury assessment in landmine detonations under a vehicle. *IUTAM Symposium on Biomechanics of Impact: From Fundamental Insights to Applications,* Dublin, Ireland. 41-49.

Huelke, D. F. (1986). Anatomy of the lower extremity - an overview. *Symposium on Biomechanics and Medical Aspects of Lower Limb Injuries,* San Diego, CA. 1-22.

Jaffredo, A. S., Potier, P., Robin, S., Le Coz, J. Y., & Lassau, J. P. (2000). Cadaver lower limb dynamic response in inversion-eversion. *2000 International IRCOBI Conference,* Montpellier, France. 183.

Khan, W., Oragui, E., & Akagha, E. (2010). Common fractures and injuries of the ankle and foot: Functional anatomy, imaging, classification and management. *Journal of Perioperative Practice, 20*(7), 249-258.

Kitagawa, Y., Ichikawa, H., King, A. I., & Levine, R. S. (1998). A severe ankle and foot injury in frontal crashes and its mechanism. *42nd Stapp Car Crash Conference,* Tempe, AZ.

Klopp, G. S., Crandall, J. R., Hall, G. W., Pilkey, W. D., Hurwitz, S. R., & Kuppa, S. M. (1997). Mechanisms of injury and injury criteria for the human foot and ankle in dynamic axial impacts to the foot. *1997 International IRCOBI Conference,* Hannover, Germany. 73-86.

Klopp, G. S., Crandall, J. R., Hurwitz, S. R., Pilkey, W. D., Morgan, R. M., Eppinger, R. H., & Kuppa, S. M. (1995). Risk of injury to the human ankle for longitudinal impacts to the foot. *International Conference on Pelvic and Lower Extremity Injuries,* Washington, DC. 233-245.

Kuppa, S. M., Klopp, G. S., Crandall, J. R., Hall, G. W., Yoganandan, N., Pintar, F. A., . . . Kleinberger, M. (1998). Axial impact characteristics of dummy and cadaver lower limbs. *16th International Technical Conference on the Enhanced Safety of Vehicles,* Windsor, Ontario, Canada. 1608-1617.

Kuppa, S. M., Wang, J., Haffner, M. P., & Eppinger, R. H. (2001). Lower extremity injuries and associated injury criteria. *17th International Technical Conference on the Enhanced Safety of Vehicles,* Amsterdam, the Netherlands.

Lauge-Hansen, N. (1950). Fractures of the ankle. II. Combined experimental-surgical and experimental-roentgenologic investigations. *Archives of Surgery, 60*(5), 957-985.

Lessley, D., Crandall, J., Shaw, G., Kent, R., & Funk J. (2004). A normalization technique for developing corridors from individual subject responses. SAE Technical Paper 2004-01-0288.

Manning, P., Wallace, W. A., Owen, C., Roberts, A. K., Oakley, C., & Lowne, R. W. (1998). Dynamic response and injury mechanism in the human foot and ankle and an analysis of dummy biofidelity. *16th International Technical Conference on the Enhanced Safety of Vehicles,* Windsor, Ontario, Canada. 1960-1998.

Manning, P., Wallace, W. A., Roberts, A. K., Owen, C., & Lowne, R. W. (1997). The position and movement of the foot in emergency maneuvers and the influence of tension in the Achilles tendon. *41st Stapp Car Crash Conference,* Warrendale, PA. 195-206.

Manseau, J., & Keown, M. (2005). Development of an assessment methodology for lower leg injuries resulting from anti-vehicular blast landmines. *IUTAM Symposium on Biomechanics of Impact: From Fundamental Insights to Applications,* Dublin, Ireland. 33-40.

McKay, B. J. (2010). Development of lower extremity injury criteria and biomechanical surrogate to evaluate military vehicle occupant injury during an explosive blast event. (Unpublished PhD). Wayne State University,

McKay, B. J. & Bir, C. A. (2009). Lower extremity injury criteria for evaluating military vehicle occupant injury in underbelly blast events. *Stapp Car Crash Journal, 53*, 229-249.

McMaster, J., Parry, M., Wallace, W. A., Wheeler, L., Owen, C., Lowne, R. W. . . . Roberts, A. K. (2000). Biomechanics of ankle and hindfoot injuries in dynamic axial loading. *44th Stapp Car Crash Conference,* Atlanta, GA.

NATO Research and Technology Organization. (2007). Test methodology for protection of vehicle occupants against anti-vehicular landmine effects. (No. AC/323(HFM-090)TP/72).

Office of the Under Secretary of Defense. (2011). Population representation in the military services: Fiscal year 2011 summary report.

Owens, B. D., Kragh, J. F., Jr., Macaitis, J., Svoboda, S. J., & Wenke, J. C. (2007). Characterization of extremity wounds in Operation Iraqi Freedom and Operation Enduring Freedom. *Journal of Orthopaedic Trauma, 21*(4), 254-257.

Pandelani, T., Reinecke, D., Philippens, M., Dosquet, F., & Beetge, F. (2010). The practical evaluation of the Mil-Lx lower leg when subjected to simulated vehicle under belly blast load conditions. *Personal Armour Systems Symposium,* Quebec City, Quebec, Canada. 1-10.

Parenteau, C. S., Viano, D. C., & Lovsund, P. (1995). Foot and ankle injury epidemiological and biomechanical studies. *International Conference on Pelvic and Lower Extremity Injuries,* Washington, DC. 191-200.

Petit, P., Portier, L., Foret-Bruno, J. Y., Trosseille, X., Parenteau, C. S., Coltat, J. C., . . . Lassau, J. P. (1996). Quasistatic characterization of the human foot and ankle joints in a simulated tensed state and updated accidentological data. *1996 International IRCOBI Conference,* Dublin, Ireland. 363-376.

Portier, L., Petit, P. Y., Domont, A., Trosseille, X., Le Coz, J. Y., Tarriere, C., & Lassau, J. P. (1997). Dynamic biomechanical dorsiflexion responses and tolerances of the ankle joint complex. *41st Stapp Car Crash Conference,* Lake Buena Vista, FL. 207-224.

Portier, L., Petit, P. Y., Trosseille, X., Tarriere, C., & Lavaste, F. (1995). Experimental research program on lower leg injuries in frontal car crashes. *International Conference on Pelvic and Lower Extremity Injuries,* Washington, DC. 173-189.

Radonic, V., Giunio, L., Biocic, M., Tripkovic, A., Lukcic, B., & Primorac, D. (2004). Injuries from antitank mines in southern Croatia. *Military Medicine, 169*(4), 320-324.

Rasmussen, O., & Tovborg-Jensen, I. (1981). Anterolateral rotational instability in the ankle joint. An experimental study of anterolateral rotational instability, talar tilt, and anterior drawer sign in relation to injuries to the lateral ligaments. *Acta Orthopaedica Scandinavica, 52*(1), 99-102.

Rudd, R. W., Crandall, J. R., Millington, S., Hurwitz, S. R., & Hoglund, N. (2004). Injury tolerance and response of the ankle joint in dynamic dorsiflexion. *Stapp Car Crash Journal, 48*, 1-26.

Sanders, R. W., & Clare, M. P. (2007). Fractures of the calcaneus. In M. J. Coughlin, R. A. Mann & C. L. Saltzman (Eds.), (8th ed., pp. 2017-2074). Philadelphia, PA: Mosby.

Sanders, R. W., & Lindvall, E. (2007). Fractures and fracture-dislocation of the talus. In M. J. Coughlin, R. A. Mann & C. L. Saltzman (Eds.), *Surgery of the foot and ankle* (8th ed., pp. 2075-2136). Philadelphia, PA: Mosby.

Sanders, R. W., & Papp, S. (2007). Fractures of the midfoot and hindfoot. In M. J. Coughlin, R. A. Mann & C. L. Saltzman (Eds.), *Surgery of the foot and ankle* (8th ed., pp. 2199-2235). Philadelphia, PA: Mosby.

Sanders, R. W., & Walling, A. K. (2007). Pilon fractures. In M. J. Coughlin, R. A. Mann & C. L. Saltzman (Eds.), *Surgery of the foot and ankle* (8th ed., pp. 1941-1972). Philadelphia: Mosby.

Schueler, F., Mattern, R., Zeidler, F., & Scheunert, D. (1995). Injuries of the lower legs - foot, ankle joint, tibia; mechanisms, tolerance limits, injury - criteria evaluation of a recent biomechanic experiment series. *1995 International IRCOBI Conference,* Brunnen, Switzerland. 33-45.

Walling, A. K., & Sanders, R. W. (2007). Ankle fractures. In M. J. Coughlin, R. A. Mann & C. L. Saltzman (Eds.), *Surgery of the foot and ankle* (8th ed., pp. 1973-2016). Philadelphia, PA: Mosby.

Wang, J., Bird, R., Swinton, B., & Krstic, A. (2001). Protection of lower limbs against floor impacts in army vehicles experiencing landmine explosion. *Journal of Battlefield Technology, 4*(3), 9-12.

Wolff, K. S., Prusa, A. M., Wibmer, A., Rankl, P., Firbas, W., & Teufelsbauer, H. (2005). Effect of body armor on simulated landmine blasts to cadaveric legs. *JTrauma, 59*(1), 202-208.

Yoganandan, N., Pintar, F. A., Boynton, M., Begeman, P. C., Prasad, P., Kuppa, S. M., & Eppinger, R. H. (1996). Dynamic axial tolerance of the human foot and ankle complex. *40th Stapp Car Crash Conference,* Albuquerque, NM. 207-218.

Yoganandan, N., Pintar, F. A., Gennarelli, T. A., Seipel, R. C., & Marks, R. M. (1999). Biomechanical tolerance of calcaneal fractures. *43rd Annual AAAM Conference,* Barcelona, Spain. 345-356.